DOI: 10.1534/genetics.110.123232

Discovery of Mutations in *Saccharomyces cerevisiae* by Pooled Linkage Analysis and Whole-Genome Sequencing

Shanda R. Birkeland,* Natsuko Jin,† Alev Cagla Ozdemir,‡ Robert H. Lyons, Jr.,§ Lois S. Weisman† and Thomas E. Wilson*,‡,1

**Department of Pathology,* †*Department of Cell and Developmental Biology, Life Sciences Institute,* ‡*Department of Human Genetics,* §*Department of Biological Chemistry and University of Michigan DNA Sequencing Core, University of Michigan Medical School, Ann Arbor, Michigan 48109*

Manuscript received July 23, 2010
Accepted for publication September 25, 2010

ABSTRACT

Many novel and important mutations arise in model organisms and human patients that can be difficult or impossible to identify using standard genetic approaches, especially for complex traits. Working with a previously uncharacterized dominant *Saccharomyces cerevisiae* mutant with impaired vacuole inheritance, we developed a pooled linkage strategy based on next-generation DNA sequencing to specifically identify functional mutations from among a large excess of polymorphisms, incidental mutations, and sequencing errors. The *VAC6-1* mutation was verified to correspond to *PHO81-R701S*, the highest priority candidate reported by VAMP, the new software platform developed for these studies. Sequence data further revealed the large extent of strain background polymorphisms and structural alterations present in the host strain, which occurred by several mechanisms including a novel Ty insertion. The results provide a snapshot of the ongoing genomic changes that ultimately result in strain divergence and evolution, as well as a general model for the discovery of functional mutations in many organisms.

THE *Saccharomyces cerevisiae* genome sequence was completed in 1996 and represented the first complete eukaryotic genome (Cherry *et al.* 1997). It was a revolutionary tool for yeast researchers and provided a model for functional genome analyses in all organisms. Something it did not routinely allow, however, was the interrogation of additional strains for novel mutations. Identification of functional mutations arising spontaneously or in screens still relies primarily on classical techniques such as linkage analysis and plasmid complementation that are effective but cumbersome and can fail with dominant mutations, large genes, and when extragenic suppressors are common. The challenges of identifying target mutations are only magnified in obligatory diploid organisms with larger and more complex genomes such as mammals.

Comprehensive and unbiased discovery of new or interesting genetic differences requires the repeated application of DNA sequencing on the whole-genome scale, which for many years remained outside the reach of experimentalists. The advent of high-throughput short-read sequencing technologies has dramatically changed this status quo. The common basis of most of these new sequencing platforms is the physical separation of single DNA molecules into an array, typically with *in situ* amplification to increase the signal yield, followed by various chemistries to reveal the base-by-base sequence at each array position using advanced imaging techniques (Metzker 2010). Platforms now allow >100 Gb of sequence to be obtained in a single run in the form of millions of reads of <100 bp. Although generally insufficient to assemble a genome *de novo*, such short reads can be mapped to a reference genome, allowing differences between the study sample and the reference sequence to be identified.

Despite their raw power, there are still many obstacles to realizing the experimental utility of short-read sequencing technologies. The first is the need for efficient computational tools to deal with the large amount of generated data. Moreover, the accuracy of current short-read technologies is lower than standard sequencing so one must sort out real mutations from sequencing errors. When the experimental goal is to discover the mutation associated with a specific phenotype, one will also need to distinguish the causative allele from other mutations that are present. Finally, chromosomal alterations such as translocations operate on an inherently larger scale than <100-bp reads, and variant approaches are required to identify them.

In this study, we sought to establish approaches to genome sequencing via short-read technologies that would satisfy the above needs. We started with an uncharacterized yeast mutant with impaired vacuole

Supporting information is available online at http://www.genetics.org/cgi/content/full/genetics.110.123232/DC1.

[1] *Corresponding author:* Department of Pathology, University of Michigan Medical School, 2065 BSRB, 109 Zina Pitcher Place, Ann Arbor, MI 48109-2200. E-mail: wilsonte@umich.edu

inheritance, *VAC6-1* (Gomes de Mesquita *et al.* 1996). We describe how genetic linkage in a single backcross was exploited to rapidly identify the *VAC6-1* allele from among >10,000 other strain mutations and polymorphisms. To maximize information quality and yield, data were generated using mate-pair technology in which both ends of genomic DNA fragments are sequenced (Dew *et al.* 2005; Korbel *et al.* 2007), which allowed a nearly complete description of the structural alterations present. Together, the results provide broadly applicable computational tools and approaches to mutation identification whose logic is readily extendable to higher eukaryotes with appropriate modifications. In addition, the comprehensive analysis of genome alterations in our strain provides a snapshot of the striking genetic differences present in laboratory organisms.

MATERIALS AND METHODS

Yeast strains: The yeast strains used in this study were obtained from the strain archive of the Weisman laboratory. JBY009/*VAC6-1* was the kind gift of Daniel Gomes de Mesquita and Conrad Woldringh (Gomes de Mesquita *et al.* 1996). To perform the screen for *VAC* mutants, the *PEP4* gene had first been knocked out of SEY6210 (*MAT*α *ura3-52 his3*-Δ*200 leu2-3,112 lys2-801 trp1*-Δ*901 suc2*-Δ*9*) to generate RHY6210 (SEY6210 *pep4*-Δ*1137*). SEY6210 itself (Robinson *et al.* 1988) was derived by crossing strains from the laboratories of Gerald Fink, Ronald Davis, David Botstein, Fred Sherman, and Randy Schekman and is commonly used in laboratories that study vacuole-related processes (see http://wiki.yeastgenome.org/index.php/Commonly_used_strains). JBY009 (RHY6210 *VAC6-1*) was the product of a screen in which RHY6210 was mutagenized with UV irradiation (254 nm, 1 J m^{-2}, 20 sec) to 40% viability (Gomes de Mesquita *et al.* 1996). For backcrossing, we introduced plasmid pGAL-HO into a *PEP4* version of a strain that we believed to be otherwise isogenic with RHY6210 to generate a *MAT***a** strain that was used as the backcross parent. Eight dissected asci from a first backcross of JBY009 had been archived and were recovered from the freezer for sequencing. The yeast used to demonstrate the detection of structural variations were from the wild-type segregant pool obtained from sporulation of diploid strain LWY10741 (*MAT***a**/α *ura3-52*/*ura3-52 his3*-Δ*200*/*his3*-Δ*200 leu2-3,112*/*leu2-3,112 lys2-801*/*lys2-801 trp1*-Δ*901*/*trp1*-Δ*901 suc2*-Δ*9*/*suc2*-Δ*9 VAC22*/*vac22-1*), which also derived from SEY6210.

Pooling and sequencing: The statistical assessments and modeling used to derive the probabilities of identifying causative mutations and excluding incidental mutations are described in supporting information, Materials and Methods, File S1. Because the pooled linkage strategy assumes equal representation of all segregants in a pool, we took special care when making genomic DNA. All spore clones obtained from the eight dissected *VAC6-1* heterozygous asci were grown overnight at 30° in individual 25-ml YPAD cultures (1% yeast extract, 2% peptone, 40 μg/ml adenine, 2% dextrose). The OD_{600} of the cultures was determined and used to calculate the appropriate volume of each strain to mix to achieve equal numbers of cells. Pools were made for the wild-type and mutant strains and genomic DNA was prepared without further outgrowth. Wild-type and mutant mate-pair libraries were made using the Illumina Mate Pair Library Prep Kit according to the manufacturer's instructions. Briefly, the process entailed shearing genomic DNA to ~3-kb fragments and preparing the two fragment ends for sequencing via steps including circularization, reshearing, ligation of sequencing adapters, and limited PCR (see Figure S1 in File S1). Paired-end sequencing was finally performed on the Illumina Genome Analyzer by the University of Michigan DNA Sequencing Core. Sequence image analysis and base calling were performed using the Illumina Firecrest and Bustard algorithms, respectively, according to the instructions. All called sequence reads are available in FASTQ format from the National Center for Biotechnology Information Sequence Read Archive under submission SRA023658, study SRP003355.

Mutation finding: All subsequent sequence data analyses were performed using the informatics platform that we developed called VAMP, for Visualization and Analysis of Mate-Pairs, which is available for download at http://tewlab.path.med.umich.edu/vamp.html. The methods and logic used by VAMP are described in SI Material and Methods and Figure S1, Figure S2, Figure S3, and Figure S4 in File S1. Mapping was performed using the PASS program (Campagna *et al.* 2009), which supports the identification of small indels in addition to point mutations, as coordinated by the VAMP wrapper. The reference genome was the 2003 release of the *S. cerevisiae* genome (sacCer2). Mapping filters allowed up to five discrepancies (mismatches or indels) relative to sacCer2 and up to 10 initial genome map positions. Best mappings were chosen by giving priority to those mate-pairs with the expected separation of ~3 kb or those consistent with the orientation artifact described in Figure S1 in File S1. Candidate *VAC6-1* causative alleles were defined as sequence alterations that showed: (i) a predicted coding change in a yeast gene, (ii) at least three crossing reads in each of the wild-type and mutant pools, (iii) no more than 10% of wild-type pool reads consistent with the mutation, and (iv) at least 90% of mutant pool reads consistent with the mutation. To find Ty elements inserted relative to sacCer2, we used VAMP's modified mapping algorithm (see SI Materials and Methods, File S1) with the panel of all known yeast Ty elements as the training set. Implicated Ty reads were assembled into a contig by iterative refinement against known Ty sequences.

Validation of the *VAC6-1* allele: A 5.7-kb *PHO81* DNA fragment (−1695 to 4062 bp) from wild-type or *VAC6-1* genomic DNA was subcloned into the *Sac*II and *Sal*I sites of pRS413 (*CEN*, *HIS*3) by fusing four tandem PCR fragments. Yeast strain LWY7235 (*MAT***a** *leu2-3,112 ura3-52 his3*-Δ*200 trp1*-Δ*901 lys2-801 suc2*-Δ*9*) (Bonangelino *et al.* 1997) was transformed with these plasmids or pRS413 and cells labeled with the fluorescent dye FM4-64 for microscopic visualization of the vacuole (Vida and Emr 1995).

RESULTS

Linkage analysis by sequencing bulk segregants: To identify the genetic alteration underlying an observable yeast phenotype by genome sequencing, the causative mutation must be both positively identified and distinguished from sequencing errors, strain polymorphisms, and, in the case of a screen isolate, noncausative mutations incidentally induced by the source mutagen. We considered two strategies for achieving these goals (Figure 1). In the first, standard serial backcrossing of the mutant strain is performed against an isogenic wild-type strain, selecting a single segregant that displays the

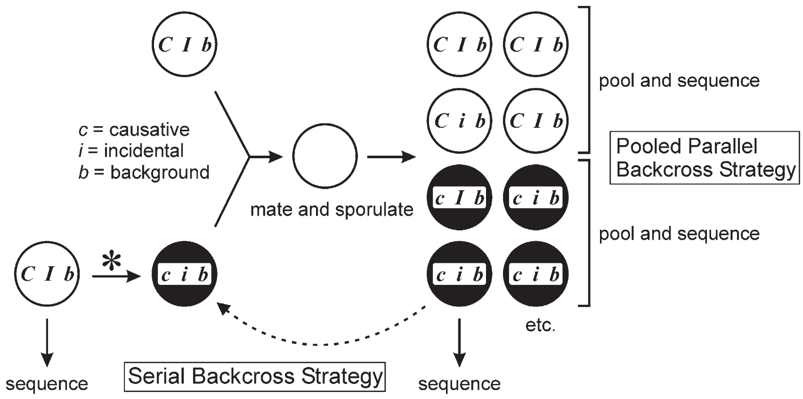

FIGURE 1.—The pooled parallel backcross strategy. In the scenario depicted, a yeast strain with a novel phenotype (indicated by a solid circle) is derived by mutagenesis of a parental wild-type strain (indicated by an open circle). The mutant is backcrossed against the parental strain and asci are scored. In the serial backcross strategy, this process is repeated until a single mutant segregant is ultimately chosen for sequencing. In the pooled parallel backcross strategy, all wild-type and all mutant segregants from several asci from the first backcross are pooled and sequenced in two separate libraries. Letters indicate the three classes of mutation that must be tracked. *C*/*c* refers to wild-type and mutant alleles of the gene bearing the *c*ausative mutation, which by definition always cosegregates with the mutant phenotype. *I*/*i* refers to an unlinked *i*ncidental mutation induced by EMS, which will sort randomly with respect to the phenotype. *B*/*b* refers to a mutation present in the strain *b*ackground prior to EMS mutagenesis.

mutant phenotype at each cross. Sequencing is ultimately applied to the last selected mutant segregant and the parent strain. The alternative approach, which we employed, entails a single backcross with many asci obtained in parallel. Instead of sequencing pure clonal isolates, all mutant segregants from a series of asci are pooled and bulk genomic DNA and a corresponding library are prepared and sequenced. The pool of all wild-type segregants from the same asci is sequenced in parallel for the same total of two required sequencing runs as the serial backcross strategy.

The net result of the pooled parallel backcross strategy, also known as "bulk segregants" (BRAUER *et al.* 2006; EHRENREICH *et al.* 2010; WENGER *et al.* 2010), is a powerful linkage experiment (Figures 1 and 2). Tight linkage and presumed possible causality are revealed by mutations that are present in 100% of mutant pool and 0% of wild-type pool sequence reads. Unlinked incidental mutations as well as sequencing errors are expected to yield a mixture of wild-type and mutant bases in both the wild-type and the mutant pools. Strain background polymorphisms will be present in 100% of reads in both pools, assuming that an isogenic wild-type strain is used in the backcross. If an isogenic strain is not used, differences between the mated strains will again sort between wild-type and mutant pools at a frequency consistent with their degree of linkage to the causative allele.

Figure 2 compares the statistical power of the serial and parallel approaches. Serial backcrosses have relatively low discriminatory power for the exclusion of incidental mutations over the range of backcross iterations typically used by most yeast researchers. Pooled parallel backcrosses have much greater discriminatory power mainly because the total information content of every ascus can be brought to bear in the analysis. Surprisingly, few asci need to be sampled to exclude the large majority of incidental mutations, mainly because the probability of selecting only parental ditype asci rapidly becomes very small. The power is dependent on the sequence coverage obtained, but Figure 2 demonstrates that 10-fold genome coverage of each pool is sufficient to capture nearly all of the available information. Critically, at 10-fold coverage the probability that the causative mutation will be sequenced by at least three independent reads is 0.997 (0.875 and 1.000 for 5- and 25-fold coverage, respectively). This is severalfold less coverage than provided by a single Illumina sequencing lane (Table 1).

Point mutation content of the *VAC6-1* mutant strain: To test the parallel backcross strategy, we applied it to identification of the *VAC6-1* mutation, which causes a defect in vacuolar inheritance scored by microscopic examination of fluorescently labeled cells (GOMES DE MESQUITA *et al.* 1996; WANG *et al.* 1996). Because *VAC6-1* is a dominant allele, it could not be identified by standard complementation cloning and thus the genetic basis of the defect was unknown. We pooled archived wild-type and mutant segregants from eight asci from the first backcross of JBY009, the *VAC6-1* strain obtained from a UV mutagenesis screen of parental strain RHY6210 (GOMES DE MESQUITA *et al.* 1996), itself a derivative of SEY6210 (ROBINSON *et al.* 1988). A 3-kb mate-pair library was prepared for each of the wild-type and mutant spore pools, and each was sequenced in a single Illumina lane using paired reads (Table 1). Sequence reads were mapped to the yeast reference genome and analyzed using the VAMP software platform. Comparison of Figure 2 to the run data in Table 1 indicated that the coverage obtained would be sufficient to both identify the *VAC6-1* mutation and to exclude all but the most closely linked incidental mutations.

Figure 3 shows a histogram of the number of sequence changes that we observed relative to S288C, the strain represented by the reference genome, according to the fractional representation in the combined wild-type and mutant pool data. This is equivalent to what would have been obtained had the backcross

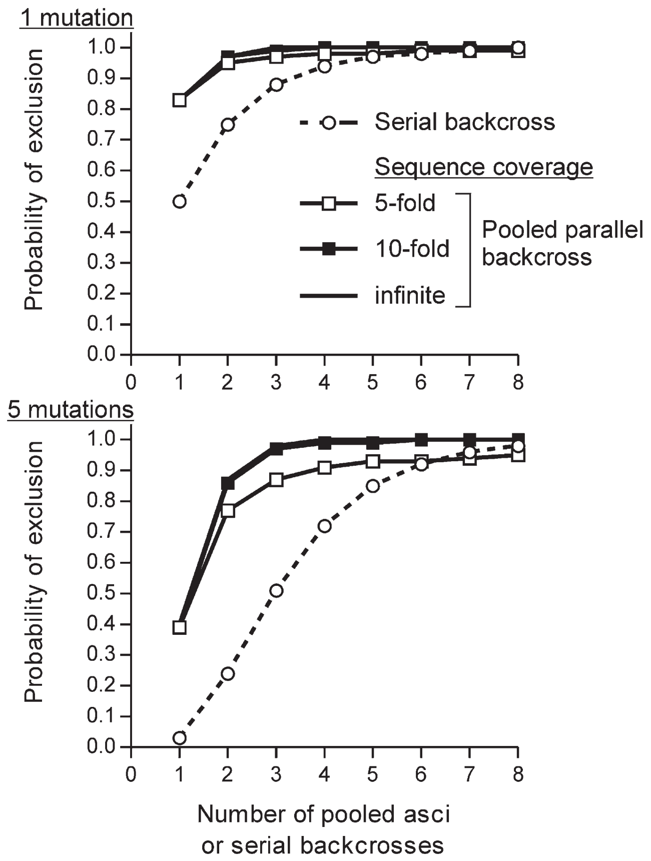

Figure 2.—Statistical power of pooled linkage analysis by sequencing. Graphs show the probability of excluding either one (top) or five (bottom) incidental mutation(s) as the causative allele as a function of the number of pooled asci (solid lines) or serial backcrosses (dashed lines with open circles). For the pooled parallel backcross strategy, an obscured solid line indicates the theoretical maximum probability of exclusion corresponding to infinitely deep sequencing of the strain pools, while solid lines with open and solid squares show the results of a 10,000-iteration simulation conducted at 5- and 10-fold average genome coverage per pool, respectively.

TABLE 1

Sequencing pool summary statistics

	VAC6-1		
	Wild type	Mutant	LWY10741
Solexa lanes	1	1	1
Read length (bp)	36	36	39
Mean fragment size (bp)	3085	2610	2799
Unique mate pairs	1.4×10^{7}	1.3×10^{7}	4.1×10^{6}
Allowed pair mappings	4.5×10^{6}	5.2×10^{6}	2.0×10^{6}
Mapped reads	9.0×10^{6}	1.0×10^{7}	4.1×10^{6}
Mean base coverage	27	31	13
Median base coverage	25	27	12
Base mismatch rate (%)	0.6	0.5	0.4

diploid itself been sequenced. Three features are evident. The first is a very large number of sequence changes substantially below the 50% frequency expected for diploid heterozygous mutations. These correspond primarily to sporadic sequencing errors, which occurred in our samples at a frequency of ∼0.5% (Table 1). More important were two peaks corresponding to ∼50% and ∼100% mutation frequencies in the combined pools, sequence changes inferred to have been heterozygous and homozygous in the backcross diploid, respectively. Strikingly, >6000 heterozygous and 4000 homozygous changes were called (see Table S1). Inspection of individual calls provided clear corroboration (see Figure S5 in File S1). Further inspection confirmed that the large majority of alterations (85%) corresponded to population polymorphisms present in at least 1 of the 38 strains sequenced by the Saccharomyces Genome Resequencing Project (Liti *et al.* 2009), with 7403 (71%) present in five or more strains. The strongest match was to laboratory strain SK1, which shared 5339 (51%) of the changes that we observed, but similarly high rates of correspondence were seen with natural *S. cerevisiae* isolates, such as RM11-1a, which shared 5076 (49%).

A strongly nonrandom distribution of both homozygous and heterozygous sequence changes was observed throughout the genome (Figure 4A). We interpret the obvious clustering of most polymorphisms as recombination blocks created by crosses that occurred previously in the history of our strains relative to S288C. Regions of low mutation density were inherited from a strain(s) closely related to S288C during the complex history that gave rise to RHY6210 and SEY6210 (Figure 4B and materials and methods). In contrast, homozygous high-density mutation blocks represent RHY6210 chromosome regions inherited from a background other than S288C. The observed heterozygous high-density mutation blocks were unexpected, however, since we had believed JBY009/*VAC6-1* and its backcross parent to be isogenic. Examination of the sequence data revealed that the SEY6210 auxotrophic markers *his3*Δ*-200*, *trp1-*Δ*901*, and *leu2-3,112* were also unexpectedly heterozygous, and indeed phenotypic testing showed the backcross parent to be His$^+$, Trp$^+$, and Leu$^+$. We thus infer that this strain had in fact been crossed to a strain more closely related to S288C prior to the manipulations that we performed (Figure 4B and materials and methods). Notably, 24% and 27% of the heterozygous and homozygous mutations, respectively, changed coding of a yeast gene (Figure 3), including nonsense mutations in *LYS2* (a known auxotrophic marker), *YFR057W*, *SIM1*, *YKL133C*, *SPH1*, *RPS22B*, *UFO1*, *YML082W*, *ISW2*, and *GRE2*, underscoring the large genetic differences that can exist between laboratory yeast strains (Liti *et al.* 2009).

***PHO81*-R701S encodes *VAC6-1*:** Although noteworthy, no high-density mutation block in Figure 4 was likely to contain the *VAC6-1* causative allele because none consistently showed the highest degree of linkage required of a causative locus. Indeed, nonsynonymous

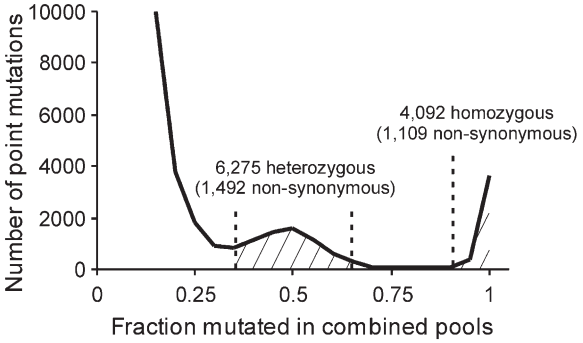

Figure 3.—Frequency distribution of observed point mutations and SNPs. Sequence data from the *VAC6* wild-type and mutant spore pools were combined to show the point mutation content in the diploid backcross strain. True sequence changes are expected to cluster in peaks at frequencies of 50% and 100%, corresponding to heterozygous and homozygous changes in the diploid strain, respectively. Frequencies need not be precisely 50% or 100% because of stochastic effects in pool sampling. Heterozygous (35–65% frequency) and homozygous (>90% frequency) mutation counts are shown. The off-scale peak of sequence changes at <25% frequency corresponds to sequencing errors.

mutations that showed at least 90% segregation into the *VAC6-1* mutant pool affected only two genes, *RPS0A* and *PHO81* (Table 2). Because these genes are near each other on chromosome VII, it was very likely that one of them was the causative allele and that the other was linked to it (Figure 4A). However, even one failed correspondence between phenotype and the candidate mutation is theoretical cause for exclusion, and neither of the candidates showed perfect segregation. This prompted us to rescore the phenotype of the segregants present in the wild-type and mutant pools, which revealed that two strains had in fact been scored incorrectly and been switched, a corruption consistent with the read frequencies in Table 2. This demonstrates the power of pooled linkage analysis even when assignment errors are possible with a complex and difficult-to-score phenotype.

Figure 4A revealed the presence of several other mutations in the *RPS0A*/*PHO81* region of chromosome VII that showed LOD scores similar to these genes but that did not appear on the candidate mutation list. Closer examination of the counts of these mutations (see Table S1) revealed that all were in fact anticorrelated to the *VAC6-1* mutant phenotype in being present in ~90% of reads from the wild type, not the mutant, pool. We infer that these mutations were on the other copy of chromosome VII in contrast to the *RPS0A* and *PHO81* mutations. This demonstrates the power of linkage for the identification of target genomic loci even when the mutations scored are not causative.

With two genes on the candidate list, final prioritization was based on function. Of the candidates, *RPS0A* encodes a ribosome component with no obvious connection to vacuole biology. Moreover, it is substantially redundant with *RPS0B* (Demianova *et al.* 1996). In marked contrast, candidate *PHO81* encodes a cyclin-dependent kinase (CDK) inhibitor that regulates the activity of the Pho80/85 CDK complex. This made *PHO81-R701S* a strong candidate since we have shown that vacuolar mutant *vac5* results from mutation of *PHO80* (Nicolson *et al.* 1995). Because *VAC6-1* is a dominant mutation, we tested our hypothesis that *PHO81-R701S* encodes *VAC6-1* by recovering the *PHO81* allele from wild-type and *VAC6-1* mutant strains, cloning them into a plasmid vector and transforming these into wild-type yeast. Introduction of the wild-type vector had no effect on vacuole inheritance whereas the *VAC6-1*-mutant *PHO81* vector precisely recapitulated the *VAC6-1* phenotype (Figure 5). Because standard sequencing of the recovered *PHO81* alleles confirmed the presence of the *R701S* mutation, we conclude that *VAC6-1* is *PHO81-R701S*.

Finding yeast structural variations: UV and EMS mutagenesis principally induce point mutations, but there are many scenarios where large-scale structural alterations of the yeast genome must be tracked. Because of technical limitations with the *VAC6-1* sequence pools (see above and Figure S1 in File S1), it is more straightforward to present these approaches using sequence obtained with a different yeast strain, LWY10741 (see materials and methods).

The ability to score structural variations depends on the use of paired reads during sequencing, as illustrated in Figure 6A and described in SI Materials and Methods according to published logic (Dew *et al.* 2005; Korbel *et al.* 2007). The concept is to identify discrepancies between the orientation and separation of paired reads inferred from genome mapping as compared to what is expected for the library. In this way, 14 genome deletions relative to sacCer2 were called for LWY10741 (Table 3; Figure 6; Figure S6, Figure S7, and Figure S8 in File S1). No insertions, inversions, or duplications were detected that were not within tandem LTR repeats, subtelomeric regions, or rDNA where mapping is untrustworthy. Three of the observed deletions were expected since *his3-Δ200* (Figure 6B), *trp1-Δ901*, and *suc2-Δ9* are known mutations in the sequenced strain, providing internal validation of the results. Because, to our knowledge, the origin and structure of *suc2-Δ9* has never been reported (Emr *et al.* 1983), we reconstructed the allele and found that it was created by a microhomology mechanism corresponding to an *Eco*RI site (see Figure S7 in File S1). The last non-Ty deletion was unanticipated but equally clear. It removed the intergenic region between *HXT6* and *HXT7*, and the read pattern demonstrated that this event occurred by homologous recombination between these nearly identical genes (Figure 6, C and D).

The remaining 10 called "deletions" all corresponded to Ty retrotransposon elements (Voytas and Boeke 1993; Kim *et al.* 1998) in the sacCer2 reference

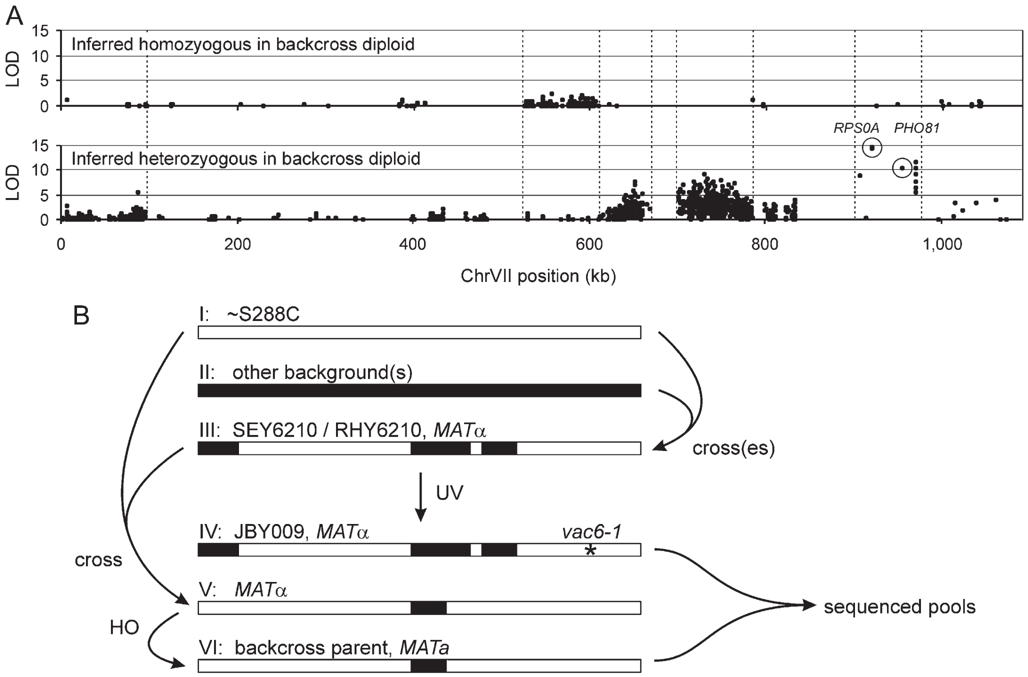

Figure 4.—Most *VAC6-1* strain mutations occur in nonrandom blocks. (A) Chromosome distribution plots were constructed for all inferred homozygous (top) and heterozygous (bottom) mutations observed in the *VAC6* wild-type and mutant pools (see Figure 3). Only chromosome VII, which contains the causative *PH081* mutation, is shown (similar trends could be observed on all chromosomes). Every mutation is plotted as a single point, although there is often insufficient resolution to visualize all loci. The *y*-axes are the linkage LOD scores for the mutation relative to the *VAC6* mutant phenotype. Mutations from the high-priority candidate list (Table 2) are circled and labeled. Vertical dashed lines indicate the edge of chromosome blocks that contain clustered mutations. (B) Drawings depict the strain history of JBY009/*VAC6-1* to illustrate the inferred origin of high-density mutation blocks from prior meiotic recombination events. For each strain, chromosome VII is depicted as open when it generally matches the S288C reference genome and as solid when a high density of non-S288C values are present. Early crosses led to the mosaic strain III used for *VAC6-1* mutagenesis. Inferred but undocumented crossing of strains I and III allowed further partial recombination of some high-density blocks in strain V and then strain VI, the strain ultimately used as the *VAC6-1* backcross parent, leading to the zygosity pattern observed in A.

sequence (Table 3). The robustness of these calls is supported by comparing the read patterns for the non-Ty deletions (Figure 6) to those seen for deleted and nondeleted Ty elements (see Figure S8 in File S1). Thus, 24% of the 50 annotated Ty elements were not present in our strain. Two equally frequent and distinct patterns were observed for the missing Ty elements (see Figure S8 in File S1). In one pattern, Ty LTRs were found to be residual at the locus, suggesting that a Ty had been present but was deleted by homologous recombination between the flanking LTRs. In the other pattern, no LTRs were apparent, which might reflect a different loss mechanism or that the Ty was never present in LWY10741.

We next asked whether our strain might contain unknown Ty elements. Importantly, an intact ~6-kb Ty is too large to be flanked by a 3-kb DNA fragment so that reads near a novel Ty will be "unpaired" (Figure 7A). We therefore wrote algorithms to establish the location of unpaired reads whose partner read could be mapped to any one of the highly related known yeast Ty elements (Figure 7B). By examining the orientation and clustering of such reads, we identified one previously unknown Ty element in our strain (Figure 7C). Assembling the sequence contig from the partner reads (see Figure S9 in File S1) showed it to be of the Ty1 family, mostly closely related to *YJRWTy1-2* with 98% sequence identity >5.5 kb. There were sequence differences relative to all known Ty elements, however. Unsurprisingly, the insertion site is within 1 kb of two tRNA genes (Figure 7C), a known feature of Ty genome locations (Bolton and Boeke 2003). Strikingly, the novel Ty is within and disrupts gene *UBC4*, which encodes a ubiquitin-conjugating enzyme (Seufert and Jentsch 1990),

TABLE 2

Nonsynonymous mutations with at least 90% segregation into the *VAC6-1* mutant pool

			Sequence pool				
Chromosome	Position(s)	Mutation	Wild type	Mutant	LOD	Gene	Mutation
VII	956,111	C to A	0/19	25/27	10.2	*PHO81*	R701S
VII	921,514 and 921,515	CC to AT	3/34	45/49	14.5	*RPS0A*	P161S

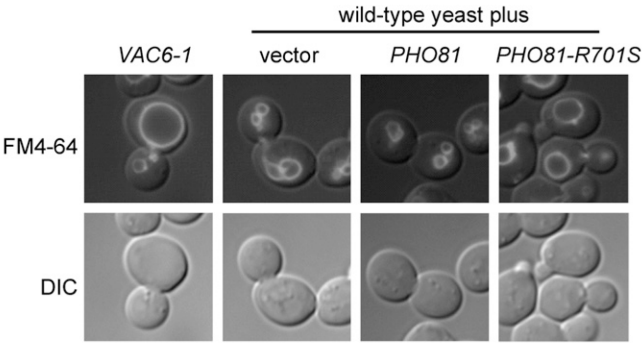

Figure 5.—*PHO81*-R701S is the causative mutation in *VAC6-1*. Transformation of wild-type yeast with either pRS413 vector or pRS413-*PHO81* had no effect on vacuole inheritance, whereas transformation with pRS413-*PHO81-R701S* caused an enlarged vacuole in the mother cell and a vacuole inheritance defect (right panels). Wild-type cells bearing pRS413-*PHO81-R701S* showed the same phenotype as *VAC6-1* itself (left).

again emphasizing the substantial genetic differences that can exist between laboratory yeast strains.

Surprisingly, the query for new Ty elements did not return the *URA3* locus. We had expected this since LWY10741 is homozygous for *ura3-52*, a well described 6-kb Ty insertion mutation (Rose and Winston 1984). Examination of *URA3* revealed that no sequence reads had mapped across the *ura3-52* insertion site (chromosome V, position 116,282), consistent with an insertion at this point, and that there were indeed Ty mate-pairs in the flanking regions (not shown). However, there were not enough such pairs to pass the threshold we used when calling Ty sets. This paucity of fragments would be explained by a small Ty insertion, which restricts the number of reads that can map within it. Accordingly, nearly all mate-pairs that spanned the Ty insertion point were individually too close to the library mean fragment size to be called as deviant, but when considered together, these 417 fragments predicted a net insertion of 278 ± 202 bp ($P = 3 \times 10^{-98}$ by the *t*-test relative to an expected insertion of 0 bp). We conclude that the LWY10741 *ura3* allele did derive from *ura3-52* but that the Ty element itself was subsequently deleted so that only a residual LTR remains.

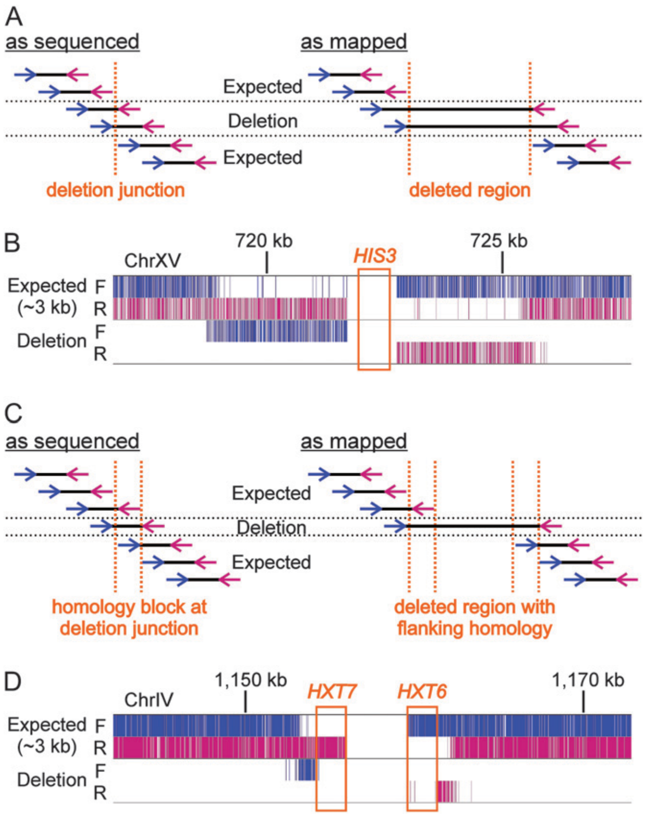

Figure 6.—Two mechanisms of chromosome deletion. (A) It is assumed that "as sequenced" all mate-pairs corresponded to $\sim$3-kb physical DNA fragments present in the strain genome. However, "as mapped" to the reference genome mate-pairs flanking a deletion junction show an excessively large spacing. (B) An example deletion corresponding to *his3-Δ200*. All expected ($\sim$3 kb) and deletion reads in both the forward (F) and reverse (R) orientations in the displayed region of chromosome XV are drawn as vertical lines. Forward and reverse read colors match the arrows in A. Although not illustrated, every forward deletion read was paired with a corresponding reverse deletion read on the opposite side of *HIS3*. The presence of a homozygous deletion is confirmed by the loss of expected reads within and surrounding the deleted segment in a pattern consistent with A. (C) Similar to A, showing the expected pattern of reads when the deletion occurs by homologous recombination via a homology block flanking the deleted locus. (D) Similar to B, showing a deletion inferred to have occurred by homologous recombination between *HXT7* and *HXT6* by the logic in C.

DISCUSSION

Identifying yeast strain mutations by pooled linkage analysis: Tracking linkage during meiotic recombination has been an invaluable technique in yeast genetic analysis for many decades (Mortimer and Hawthorne 1975; Mortimer and Schild 1985). Here, we demonstrate how to apply this concept to the efficient identification of uncharacterized mutations in light of an emergent ability to rapidly resequence the yeast genome with short-read technologies (Figure 1) (Metzker 2010). Tracking linkage in pools requires no more sequencing than other approaches and all but eliminates concerns over sequence errors and off-target mutations. Statistical modeling (Figure 2) and a practical example (Table 2 and Figure 5) confirmed that mutation identification requires only one backcross, surprisingly few asci, and little genome coverage. A similar approach also recently identified a novel xylose utilization gene (Wenger *et al.* 2010).

A main alternative to using sequencing for bulk segregant analysis is to map SNPs via microarrays to identify loci of interest (Brauer *et al.* 2006). When the goal is to identify an experimentally (UV or EMS)

TABLE 3

LWY10741 genome deletions

Chromosome	Start	End	Size (bp)	Genes affected	LTR present
IV	461,743	463,183	1441	*TRP1*	NA
IV	1,155,970[a]	1,159,523	3553	*HXT7, HXT6*	NA
IX	36,451	40,812	4361	*SUC2*	NA
XV	721,747	722,769	1023	*HIS3*	NA
II	221,045	226,969	5925	*YBLWTy1-1*	—
II	258,752	266,237	7486	*YBRWTy1-2*	Yes
IV	645,271	651,442	6172	*YDRCTy1-1*	Yes
IV	1,206,705	1,212,619	5915	*YDRWTy1-5*	—
VII	560,879	567,760	6882	*YGRCTy1-2*	—
VII	568,747	576,272	7526	*YGRCTy2-1*	—
VII	535,768	541,681	5914	*YGRWTy1-1*	Yes
XII	593,146	599,058	5913	*YLRWTy1-2*	Yes
XIII	196,329	202,193	5865	*YMLWTy1-2*	Yes
XIII	184,168	190,077	5910	*YMLWTy1-1*	—

[a] Coordinates for this event refer to the deleted intergenic region, exclusive of *HXT7* and *HXT6*. One copy of this duplicate gene pair is deleted in addition to the indicated span.

induced alteration likely to correspond to a simple point mutation, the newer sequencing approach is clearly more powerful as it can directly and positively identify the mutation. There is no need for a custom SNP array nor a backcross strain known to create extensive heterozygosity, which could have unanticipated and undesirable effects on phenotype expression. Indeed, an isogenic backcross strain is ideal since no more than a few induced mutations will likely occur within linkage distance.

The situation is different if the target mutation might be of a type difficult to discover by sequencing. Some genomic loci, such as those found in subtelomeric regions and repetitive genes, are inherently problematic (see Figure S6 in File S1). Other mutations, notably indels, are difficult because of their specific nature. For example, a 10-bp deletion would be evident only as an absence of reads crossing the variant position. Finally, target genetic differences might be associated with genes absent from the S288C reference genome, especially when the goal is to identify loci associated with phenotypes that differ between extant yeast strains (Wenger *et al.* 2010). Regardless of the reason that a mutation is difficult to discover, linkage information provided by SNP analysis can provide the key impetus for examining a regional sequence in more detail (Wenger *et al.* 2010).

SNP analysis can be comprehensively performed with sequencing (Figure 4 and Ehrenreich *et al.* 2010), so this method is still preferred over microarrays. The main decision point for most researchers will thus be whether to perform sequencing using (i) an isogenic backcross strain, ideal for simple point mutations in known genes; (ii) a backcross strain deliberately chosen to yield a large number of SNPs, ideal for linkage mapping of problematic loci (Wenger *et al.* 2010); or (iii) no backcrossing at all, ideal when the goal is to catalog all changes in a strain (Araya *et al.* 2010). Importantly, with the latter options it may not be possible to positively identify even a simple causative mutation within a linked locus, and especially not within an entire genome, due to the high density of nonsynonymous sequence alterations typically present (Figures 3 and 4) (Liti *et al.* 2009). Additional analyses can be brought to bear, including predictions of function and querying which mutations correspond to known benign polymorphisms (Ng *et al.* 2010). These assessments are weakly informative, however, as demonstrated by the fact that 15% of the sequence changes that we observed could not be accounted for by known yeast polymorphisms (Liti *et al.* 2009).

In this report, we assumed that the mutation of interest is inherited in a single-gene Mendelian fashion. However, the results give confidence that pool sequencing could also be used in the context of multigenic traits since linkage of phenotype-associated alleles will remain true as a fundamental principle. Indeed, Ehrenreich *et al.* (2010) recently exploited bulk segregant analysis in the study of multigenic quantitative trait loci. A difference is that these investigators used methods restricted to phenotypes that can be selected in pooled outgrowth cultures. Results presented here explored a complex phenotype that can be scored only individually by microscopy. Further investigation will be required to determine whether complex multigenic traits can be efficiently analyzed when only a relatively small collection of segregants can be pooled for sequencing.

For single-gene mutations, data here already demonstrate that a single Illumina sequencing lane is more than is required for a pool, and sequencing capacity is still rapidly increasing. Future efforts should thus implement multiplexing. The main approach is to use

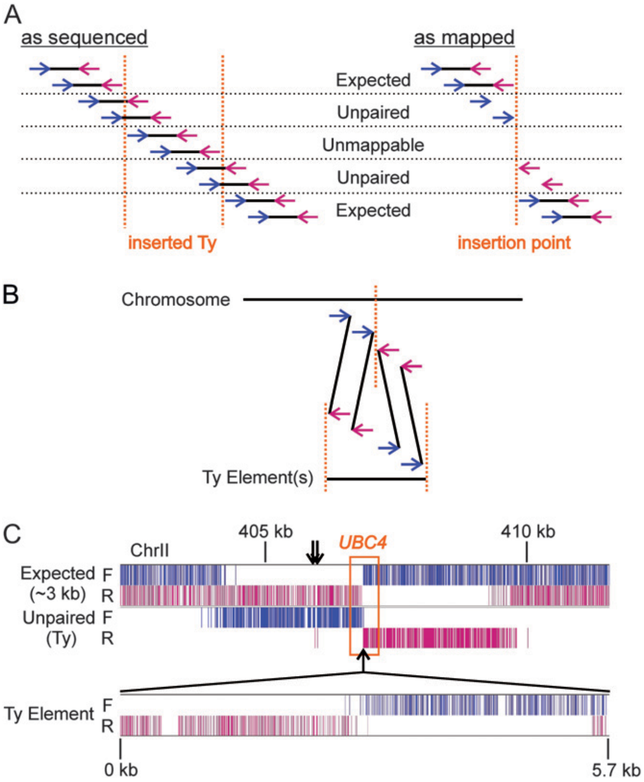

Figure 7.—A novel Ty insertion. (A) Similar to Figure 6A, showing the expected orientation of reads and fragments in the vicinity of a Ty element not present in the reference genome. (B) The strategy for identifying novel Ty insertions by comparing independent mappings of mate-pairs to (i) chromosome sequences and (ii) a training set of known Ty repeat elements. (C) An identified novel Ty insertion, illustrated as in Figure 6B, now with a track corresponding to those unpaired reads whose partners independently mapped to a Ty element(s). (Bottom) The partner reads aligned to the Ty element assembled from the data. Arrows denote the location of two closely spaced tRNA genes, *tR(UCU)B* and *tD(GUC)B*.

primers in library construction that contain fixed index sequences that identify each source sample and allow libraries to be sequenced together in a lane (Maeda *et al.* 2008). Assuming the need for 10-fold coverage, it should soon be routinely possible to sequence as many as 10 pools per lane. Importantly, it is not necessary to continue sequencing the wild-type pool for mutants derived from the same parent strain. VAMP includes algorithms to reconstruct the host genome to provide a reference for all mutants. In this way, a single lane can characterize numerous yeast mutants at a cost approaching $100 per mutant. It thus becomes practical to sequence arrays of mutants derived from a screen with minimal prior analysis.

Extension to other organisms: The pooling approach described here could be immediately applied to any organism for which the phenotypes of meiotic progeny can be assessed and for which a reference genome is available. Pooling can also be applied to organisms for which diploid offspring must be obtained to allow phenotypic assessment (Schneeberger *et al.* 2009). As an example, one could mate mice bearing a recessive mutation to wild-type individuals to create an obligatory heterozygous F_1 generation (see Figure S10 in File S1). After mating F_1 mice, a causative mutation would be present in 100% of alleles of the target gene from the pool of affected mice and in only 33% of alleles from the phenotypically normal pool.

Yeast genetic variation: To a remarkable extent, sequencing of only two related strains revealed a microcosm of the modes of genetic variation at play in yeast and other organisms (Scannell *et al.* 2007). Point mutations were the most numerous, with 10,367 called events affecting ~0.1% of the yeast genome (Figure 3). The strong bias of the mutations toward transitions (71% *vs.* a random expected frequency of 33%) was consistent with them being derived from biological mutagenesis (Sinha and Haimes 1981; Zhang and Gerstein 2003), and indeed most corresponded to known yeast SNPs (Liti *et al.* 2009). Mutations were not randomly distributed but strongly reflected the reassortment of chromosome segments via meiotic recombination (Figure 4). We also called 331 indels (see Table S1). The ratio of indels to base substitutions (0.03) is very similar to other yeast strains (0.06) (Liti *et al.* 2009), but seemingly low in the face of studies showing that indels in homopolymer runs (HPRs) are the most frequent form of spontaneous mutation (Lynch *et al.* 2008). Only 55 (17%) of our called indels were in HPRs of five or more bases, which might reflect a bias against the detection of HPR indels by short-read sequencing.

Still fewer large-scale alterations of chromosome structure were found, but because of their size one or many genes were clearly disrupted (Table 3). Each of the main modes of chromosome rearrangement (Tsai and Lieber 2010) were described by different deletions: homologous recombination within a related gene cluster (Figure 6D) and nonhomologous recombination via junctional microhomology (see Figure S7, File S1, perhaps an experimentally created alteration). Finally, we observed the ongoing role of mobile genetic elements in shaping genomes (Table 3) (Garfinkel 2005; Cordaux and Batzer 2009). The Ty content of our strain and S288C differed markedly, including (i) the apparent deletion of ancient Ty elements from our strain, evidenced by the LTR that they left behind (see Figure S8C in File S1); (ii) the possible addition of Ty elements in S288C, evidenced by their complete absence from our strain (see Figure S8A in File S1); and (iii) the addition of a Ty element to our strain, which affected it by disrupting *UBC4* (Figure 7).

***PHO81*-R701S and vacuole inheritance:** A review of the literature provides strong support for the notion that *PHO81-R701S* could have substantial impact on Pho81 function and vacuole inheritance. Pho81 is an inhibitor of the Pho80/85 CDK complex and mediates inactivation of the kinase in response to starvation for inorganic phosphate (Lenburg and O'Shea 1996). Unlike many CDK inhibitors, Pho81 remains constitutively bound to Pho80/85 (Schneider *et al.* 1994). CDK inhibition instead depends on binding of inositol heptakisphosphate (IP_7) to the complex (Lee *et al.* 2007). Dissection of the molecular interaction between Ph081 and Pho80/85 *in vitro* suggested that "minimum domain" segment 3, from residues 665 to 701, binds constitutively to Pho80/85 while minimum domain segment 1, from residues 702 to 723, binds only in the presence of IP_7 (Lee *et al.* 2008). It is thus plausible that Pho81 R701 is at the hinge point of a domain movement that occurs in response to IP_7 binding and that the *VAC6-1/PHO81-R701S* mutation alters this function. Precedent for a role of Pho80/85 signaling in vacuole inheritance is provided by the *vac5* mutant, which corresponds to a truncated allele of the Pho80 cyclin (Nicolson *et al.* 1995). Indeed, *vac5* and *VAC6* display similar vacuole morphologies. Precisely how alterations in Pho80/85 signaling lead to deregulation of vacuolar biogenesis is the subject of ongoing investigations.

We thank Emily Kaufman for assistance in recovering archived strains and scoring their phenotype and David Engelke, Anuj Kumar, Jun Li, and Thomas Glover for helpful comments on the manuscript. A. C. Ozdemir is a member of the Glover laboratory with whom the Wilson laboratory has closely collaborated in the development of human mate-pair sequencing approaches that greatly informed this project. We are grateful to the University of Michigan Depression Center for use of their computing cluster and support personnel including Fan Meng, Manhong Dai, Walter Mexner, and Tyler Brubaker. This work was supported by the University of Michigan Center for Genetics in Health and Medicine Pilot Feasibility Grant to T.E.W. and National Institutes of Health grant R01-GM050403 to L.S.W.

LITERATURE CITED

Araya, C. L., C. Payen, M. J. Dunham and S. Fields, 2010 Whole-genome sequencing of a laboratory-evolved yeast strain. BMC Genomics **11:** 88.

Bolton, E. C., and J. D. Boeke, 2003 Transcriptional interactions between yeast tRNA genes, flanking genes and Ty elements: a genomic point of view. Genome Res. **13:** 254–263.

Bonangelino, C. J., N. L. Catlett and L. S. Weisman, 1997 Vac7p, a novel vacuolar protein, is required for normal vacuole inheritance and morphology. Mol. Cell. Biol. **17:** 6847–6858.

Brauer, M. J., C. M. Christianson, D. A. Pai and M. J. Dunham, 2006 Mapping novel traits by array-assisted bulk segregant analysis in *Saccharomyces cerevisiae*. Genetics **173:** 1813–1816.

Campagna, D., A. Albiero, A. Bilardi, E. Caniato, C. Forcato *et al.*, 2009 PASS: a program to align short sequences. Bioinformatics **25:** 967–968.

Cherry, J. M., C. Ball, S. Weng, G. Juvik, R. Schmidt *et al.*, 1997 Genetic and physical maps of *Saccharomyces cerevisiae*. Nature **387:** 67–73.

Cordaux, R., and M. A. Batzer, 2009 The impact of retrotransposons on human genome evolution. Nat. Rev. Genet. **10:** 691–703.

Demianova, M., T. G. Formosa and S. R. Ellis, 1996 Yeast proteins related to the p40/laminin receptor precursor are essential components of the 40 S ribosomal subunit. J. Biol. Chem. **271:** 11383–11391.

Dew, I. M., B. Walenz and G. Sutton, 2005 A tool for analyzing mate pairs in assemblies (TAMPA). J. Comput. Biol. **12:** 497–513.

Ehrenreich, I. M., N. Torabi, Y. Jia, J. Kent, S. Martis *et al.*, 2010 Dissection of genetically complex traits with extremely large pools of yeast segregants. Nature **464:** 1039–1042.

Emr, S. D., R. Schekman, M. C. Flessel and J. Thorner, 1983 An MF alpha 1-*SUC2* (alpha-factor-invertase) gene fusion for study of protein localization and gene expression in yeast. Proc. Natl. Acad. Sci. USA **80:** 7080–7084.

Garfinkel, D. J., 2005 Genome evolution mediated by Ty elements in *Saccharomyces*. Cytogenet. Genome Res. **110:** 63–69.

Gomes de Mesquita, D. S., H. B. van den Hazel, J. Bouwman and C. L. Woldringh, 1996 Characterization of new vacuolar segregation mutants, isolated by screening for loss of proteinase B self-activation. Eur. J. Cell Biol. **71:** 237–247.

Kim, J. M., S. Vanguri, J. D. Boeke, A. Gabriel and D. F. Voytas, 1998 Transposable elements and genome organization: a comprehensive survey of retrotransposons revealed by the complete *Saccharomyces cerevisiae* genome sequence. Genome Res. **8:** 464–478.

Korbel, J. O., A. E. Urban, J. P. Affourtit, B. Godwin, F. Grubert *et al.*, 2007 Paired-end mapping reveals extensive structural variation in the human genome. Science **318:** 420–426.

Lee, Y. S., S. Mulugu, J. D. York and E. K. O'Shea, 2007 Regulation of a cyclin-CDK-CDK inhibitor complex by inositol pyrophosphates. Science **316:** 109–112.

Lee, Y. S., K. Huang, F. A. Quiocho and E. K. O'hea, 2008 Molecular basis of cyclin-CDK-CKI regulation by reversible binding of an inositol pyrophosphate. Nat. Chem. Biol. **4:** 25–32.

Lenburg, M. E., and E. K. O'Shea, 1996 Signaling phosphate starvation. Trends Biochem. Sci. **21:** 383–387.

Liti, G., D. M. Carter, A. M. Moses, J. Warringer, L. Parts *et al.*, 2009 Population genomics of domestic and wild yeasts. Nature **458:** 337–341.

Lynch, M., W. Sung, K. Morris, N. Coffey, C. R. Landry *et al.*, 2008 A genome-wide view of the spectrum of spontaneous mutations in yeast. Proc. Natl. Acad. Sci. USA **105:** 9272–9277.

Maeda, N., H. Nishiyori, M. Nakamura, C. Kawazu, M. Murata *et al.*, 2008 Development of a DNA barcode tagging method for monitoring dynamic changes in gene expression by using an ultra high-throughput sequencer. Biotechniques **45:** 95–97.

Metzker, M. L., 2010 Sequencing technologies: the next generation. Nat. Rev. Genet. **11:** 31–46.

Mortimer, R. K., and D. C. Hawthorne, 1975 Genetic mapping in yeast. Methods Cell Biol. **11:** 221–233.

Mortimer, R. K., and D. Schild, 1985 Genetic map of *Saccharomyces cerevisiae*, edition 9. Microbiol. Rev. **49:** 181–213.

Ng, S. B., K. J. Buckingham, C. Lee, A. W. Bigham, H. K. Tabor *et al.*, 2010 Exome sequencing identifies the cause of a Mendelian disorder. Nat. Genet. **42:** 30–35.

Nicolson, T. A., L. S. Weisman, G. S. Payne and W. T. Wickner, 1995 A truncated form of the Pho80 cyclin redirects the Pho85 kinase to disrupt vacuole inheritance in *S. cerevisiae*. J. Cell Biol. **130:** 835–845.

Robinson, J. S., D. J. Klionsky, L. M. Banta and S. D. Emr, 1988 Protein sorting in *Saccharomyces cerevisiae*: isolation of mutants defective in the delivery and processing of multiple vacuolar hydrolases. Mol. Cell. Biol. **8:** 4936–4948.

Rose, M., and F. Winston, 1984 Identification of a Ty insertion within the coding sequence of the *S. cerevisiae URA3* gene. Mol. Gen. Genet. **193:** 557–560.

Scannell, D. R., G. Butler and K. H. Wolfe, 2007 Yeast genome evolution: the origin of the species. Yeast **24:** 929–942.

Schneeberger, K., S. Ossowski, C. Lanz, T. Juul, A. H. Petersen *et al.*, 2009 SHOREmap: simultaneous mapping and mutation identification by deep sequencing. Nat. Methods **6:** 550–551.

Schneider, K. R., R. L. Smith and E. K. O'Shea, 1994 Phosphate-regulated inactivation of the kinase PHO80–PHO85 by the CDK inhibitor PHO81. Science **266:** 122–126.

Seufert, W., and S. Jentsch, 1990 Ubiquitin-conjugating enzymes UBC4 and UBC5 mediate selective degradation of short-lived and abnormal proteins. EMBO J. **9:** 543–550.

Sinha, N. K., and M. D. Haimes, 1981 Molecular mechanisms of substitution mutagenesis. An experimental test of the Watson-Crick and topal-fresco models of base mispairings. J. Biol. Chem. **256:** 10671–10683.

Tsai, A. G., and M. R. Lieber, 2010 Mechanisms of chromosomal rearrangement in the human genome. BMC Genomics **11** (Suppl. 1): S1.

Vida, T. A., and S. D. Emr, 1995 A new vital stain for visualizing vacuolar membrane dynamics and endocytosis in yeast. J. Cell Biol. **128:** 779–792.

Voytas, D. F., and J. D. Boeke, 1993 Yeast retrotransposons and tRNAs. Trends Genet. **9:** 421–427.

Wang, Y. X., H. Zhao, T. M. Harding, D. S. Gomes de Mesquita, C. L. Woldringh *et al.*, 1996 Multiple classes of yeast mutants are defective in vacuole partitioning yet target vacuole proteins correctly. Mol. Biol. Cell **7:** 1375–1389.

Wenger, J. W., K. Schwartz and G. Sherlock, 2010 Bulk segregant analysis by high-throughput sequencing reveals a novel xylose utilization gene from *Saccharomyces cerevisiae*. PLoS Genet. **6:** e1000942.

Zhang, Z., and M. Gerstein, 2003 Patterns of nucleotide substitution, insertion and deletion in the human genome inferred from pseudogenes. Nucleic Acids Res. **31:** 5338–5348.

Communicating editor: J. Boeke

GENETICS

Supporting Information
http://www.genetics.org/cgi/content/full/genetics.110.123232/DC1

Discovery of Mutations in *Saccharomyces cerevisiae* by Pooled Linkage Analysis and Whole-Genome Sequencing

Shanda R. Birkeland, Natsuko Jin, Alev Cagla Ozdemir, Robert H. Lyons, Jr., Lois S. Weisman and Thomas E. Wilson

DOI: 10.1534/genetics.110.123232

FILE S1

SUPPORTING MATERIAL AND METHODS

The VAMP platform. VAMP is a series of Perl scripts that create and query, via SQL, tables of short-read sequence data in an Oracle database. Visualization scripts create graphical displays in a standard web browser. VAMP scripts and extended documentation are available at http://tewlab.path.med.umich.edu/vamp.html.

Finding structural variants. VAMP first uses a logic-based approach similar to published descriptions (DEW *et al.* 2005; KORBEL *et al.* 2007) to find paired genome mappings that identify sequenced DNA fragments as either (i) corresponding to expected fragments based on the indicated reference genome and observed library fragment size or (ii) participating in a set of many fragments consistent with a structural variation not present in the reference genome.

Reference genome mapping. VAMP takes as input the called bases of paired short sequence reads, either from a standard library or a mate-pair library (Figure S1). All read pairs from all sequencing lanes for a given library are merged and identical pairs purged so that only unique pairs are subjected to mapping to the reference genome. For mapping, VAMP acts as a wrapper around the mapping programs PASS (CAMPAGNA *et al.* 2009) and Bowtie (LANGMEAD *et al.* 2009). The logic used is that the best mapping of reads in a pair can only be identified when candidate mappings can be tested against the physical DNA fragment size of the library, itself inferred from the population of all paired mappings (Figure S1). Thus, best mappings can only be determined after read mapping is completed, with the corollary that a comprehensive collection of candidate mappings must be kept until all pairs can be considered. To achieve this, VAMP coordinates the iterative mapping strategy described in Figure S2. The reference genome is not repeat masked so as to optimize the recovery of all true mappings.

Paired mappings are next examined to find the main peak from which the mean and standard deviation (SD) of the library fragment size are estimated (Figure S1). Best mappings are those falling within 3 SD of the mean. When more than one mapping is within this range, preference is given to those with fewer discrepancies and then to those closest to the mean. All other mappings for these pairs are discarded. All mappings for the remaining pairs are binned into pair types according to published logic (DEW *et al.* 2005; KORBEL *et al.* 2007), wherein inward facing pairs (after correcting read orientations, if necessary, for the inversion caused by mate-pair fragment circularization, see Figure S1) bigger than the population mean are presumptive deletions, inward facing pairs that are too small are presumptive insertions, outward facing pairs are presumptive duplications, and co-linear pairs are presumptive inversions.

Finding sets of anomalous pairs. At least two factors cause remaining anomalous pair mappings to contain many errors: chimeric ligation artifacts during library preparation and the fact that many mappings may still persist for a given pair. Thus, any inferred anomalous junction must be called independently by at least two pairs, preferably more. Moreover, the different paired mappings crossing a putative junction must satisfy the distance constraints described in Figure S3. VAMP threads the genome seeking sets of fragments of each type (deletion, etc.) consistent with these restrictions at both the left and right ends of the fragment set. Threading is achieved by examining the end positions of anomalous mappings in genome order and adding them to a growing set until the constraints described in Figure S3 are violated. When a pair gives rise to more than one mapping that participates in a set, preference is given to the mapping with the fewest discrepancies. Final validation of all inferred structural variant sets is done manually within the VAMP browser interface by user marking based on visual inspection of all pairs mapping within the given genome region.

Finding ectopic sequence insertions. Sequence insertions relative to the reference genome are a distinct mapping challenge in that two junctions are present but one end of each of the fragment sets crossing these junctions lands in DNA that is either unknown or comes from another site. One special case is the insertion of a repetitive genome element. To find such insertions, VAMP uses a modified algorithm in which pairs are first mapped to a collection of training sequences corresponding to all known repeat elements of a specific class (Figure 7B). Any pair that has exactly one read map to at least one training sequence is kept and the partner read is mapped to the entire reference genome. One-ended sets are sought among the partner read mappings by the logic above. Finally, pairs of sets are identified that are separated by a specified maximum distance and that flank a genomic locus not annotated to contain the repeat element class.

Finding point mutations and indels. The steps described above are always performed first even when the goal of the analysis is to find small sequence discrepancies (point mutations and indels). This is because the preferred method for selecting the best mapping for each individual read of a pair is to establish the best paired mapping. Specifically, only those mapped pairs corresponding to expected genomic DNA fragments or those within marked anomaly sets are used for discrepancy finding. All other mapping information is discarded as unreliable. The discrepancies relative to the reference genome for each kept read, as reported by the mapping program, are then codified and collated into an Oracle data table. When comparing samples, tables columns are created for each sample along with calculated comparative values including a LOD score. Queries executed via the browser interface then return lists of mutations satisfying thresholds such as the fraction mutated in each pool. See Figure S4 for details on a confounder that arises during discrepancy calling with short read sequence data, in which the presence of indels can lead to incorrect mismatch calls as well as under-calling of indels. These corrections were not necessary in the case of *VAC6*-1 because the mutation proved to be a simple mismatch but would be essential if the target mutation was an indel.

Backcross strategy probability calculations. When a single phenotypically mutant haploid segregant is selected from a backcross against a wild-type strain, by definition it must carry causative mutation *c*. The probability of observing *c* upon strain or pool sequencing is calculated from the average genome read coverage for the sequencing run as the sum of frequencies in the Poisson distribution corresponding to at least 3-fold coverage, the minimum number of reads required to confidently call a mutation.

Fifty percent of mutant segregants will also retain a given unlinked incidental mutation *i*. The probability of retaining *i* after *n* serial backcrosses, and thus failing to exclude it as a possible causative mutation, is 0.5^n. The probability of successfully segregating and rejecting *i* is $1 - 0.5^n$, and the probability of successfully segregating each of *m* such incidental mutations is $(1 - 0.5^n)^m$. The relationship $(1 - 0.5^n)^m$ also represents the probability that at least one of *n* spore clones each picked from different asci from the same parent diploid (i.e. parallel backcrosses) will successfully segregate each of *m* incidental mutations. The relationship does not change if one instead picks phenotypically wild-type clones since segregation is equally revealed by the presence of mutant allele *i* in a wild-type strain or wild-type allele *I* in a mutant strain.

When all four spore progeny of an ascus are tested they are no longer independent. Thus, the probability of failing to observe segregation of *i* when testing all spores of an ascus reduces to the probability that the ascus was of the uninformative parental ditype, i.e. 1/6 or 0.167, since non-parental ditype and tetratype asci all have informative spores. The probability of observing segregation when testing all spores (corresponding to infinite sequence coverage of a pool) from *a* asci is $1 - 0.167^a$, or $(1 - 0.167^a)^m$ for *m* incidental mutations.

Critically, one must actually sequence locus *I* in all pooled segregants for the above relationships to be realized. To determine the required coverage and number of pooled asci, we performed a 10,000 iteration simulation in which *a* asci were randomly chosen from the six possible ascus types (one parental ditype, one non-parental ditype and four tetratype) for each iteration. Spore counting yielded the frequency *u* of uninformative spores that failed to segregate locus *I* from the mutant phenotype in an iteration. The Poisson distribution was next used to calculate *p(s)*, the probability of observing exactly *s* sequence reads crossing *I* for a given average pool coverage *S*, for each value of *s* from 0 to 10*S*, taking into account the fact that the total effective coverage is actually twice *S* since two pools are sequenced. The probability that that all *s* sequence reads would be uninformative was calculated as u^s, and the probability of failing to segregate *I* in the iteration as the sum of the products of *p(s)* and u^s over all values of *s*. This value was averaged over all iterations to give the final estimated probability of failing to exclude *i* as a candidate causative mutation for the given values of *a* and *S*.

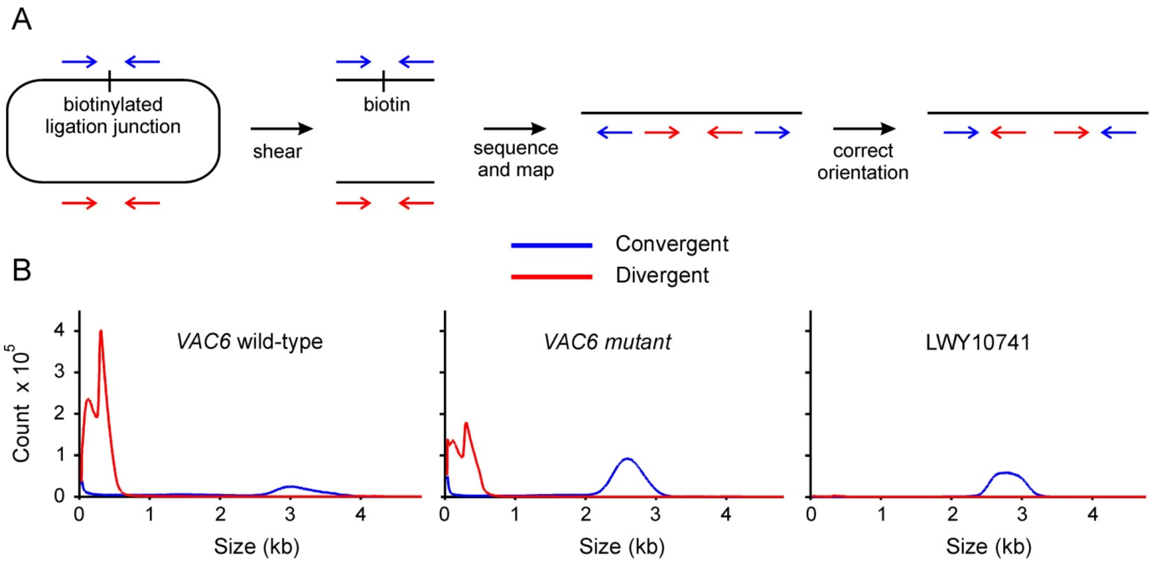

FIGURE S1.—Fragment content of the sequenced libraries. (A) Drawings depict the mate-pair process in which genomic DNA fragments are circularized and sheared prior to purification of the ligation junctions via an added biotin tag (blue arrows). Purified fragments are sequenced at both ends, and the orientation of the reads computationally reversed to correct for the inversion that occurred during circularization. However, some fragments may be carried through that did not cross a ligation junction (red arrows). Here, orientation correction is not appropriate and results in the appearance of closely spaced pair mappings in the Divergent orientation in which reads paradoxically point away from each other. (B) The Convergent (inward facing) and Divergent pair counts in the three reported libraries as a function of mapped fragment size. The two *VAC6* pools displayed much more orientation artifact, which severely limited their use in structural analysis. Importantly, this artifact has no impact on point mutation discovery because all involved mate-pairs still correspond to random reference-consistent genomic DNA fragments. Accordingly, we included the main Divergent pairs peak in the *VAC6-1* point mutation analysis.

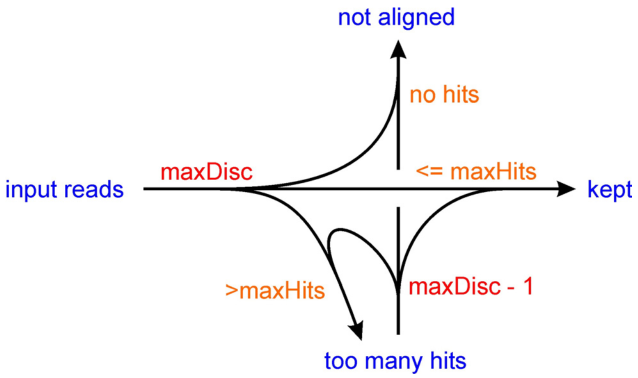

FIGURE S2.—Pair mapping strategy. Initially, VAMP accepts read mappings with no more discrepancies (mismatches plus indels) than allowed by parameter *maxDisc*. It accepts all mappings from a read pair if it finds no more mappings than allowed by parameter *maxHits*. Unmapped reads are discarded, while reads with too many mappings are attempted again with one fewer allowed discrepancies. Reads with too many mappings at even zero discrepancies are discarded.

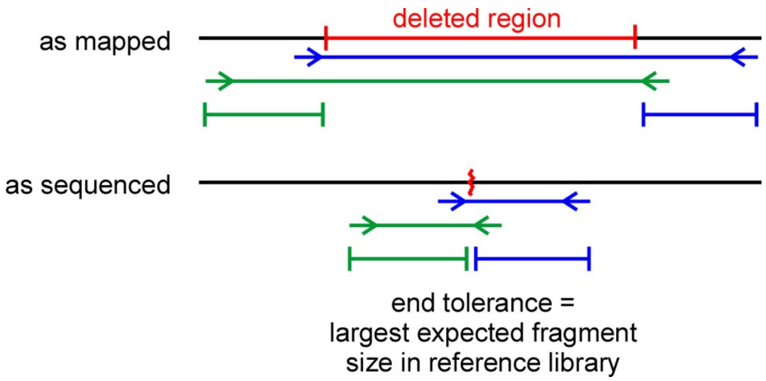

FIGURE S3.—Distance constraints in anomaly set finding. Drawings show the expected configuration of read pairs surrounding a deletion junction as it was sequenced (bottom panel) and as it was mapped to the reference genome (top panel). All DNA fragments that form a true set must overlap and therefore each group of mapped ends on the left and right sides is allowed no more separation than the mean + 3 SD of the reference library fragment size, with colors denoting the relevant reference sample for each side. Similar logic is applied to other anomaly types.

```
A

reference sequence
GAGAATCGATCCCAGATCCAGCATACGACATCGCAAATCGGGAAATCCGATCGAGCAGGGACTCT
              -------------------A--TCG--A--TC-GAT  direct map rejected
              GATCCAGCATACGACATCGAAATCGGGAAATCCGAT  read sequence
GAGAATCGATCCCAGATCCAGCATACGACATCGAAATCGGGAAATCCGATCGAGCAGGGACTCT
actual sequence


reference sequence
GAGAATCGATCCCAGATCCAGCATACGACATCGCAAATCGGGAAATCCGATCGAGCAGGGACTCT
              -------------------M-----------------  indel accepted
              GATCCAGCATACGACATCG AAATCGGGAAATCCGAT  read sequence
GAGAATCGATCCCAGATCCAGCATACGACATCG AAATCGGGAAATCCGATCGAGCAGGGACTCT
actual sequence


B

reference sequence
GAGAATCGATCCCAGATCCAGCATACGACATCGCAAATCGGGAAATCCGATCGAGCAGGGACTCT
---------------------------------A--  direct map accepted with one mismatch
GAGAATCGATCCCAGATCCAGCATACGACATCGAAA  read sequence
GAGAATCGATCCCAGATCCAGCATACGACATCGAAATCGGGAAATCCGATCGAGCAGGGACTCT
actual sequence
```

FIGURE S4.—Base calling errors near indels. Hypothetical sequences show a base, in red, that is present in the reference genome but absent in the sequenced genome. In (A), the base is in the middle of a read. Direct mapping to the genome results in an excessive number of mismatches to one side and therefore rejection of the mapping. If the mapping program is capable, it might recognize that insertion of a gap (labeled M for Missing) will allow alignment of the read with only one discrepancy. In (B), the missing base is near the end of a read. Because direct mapping generates only a single mismatch it is accepted, leading to a false apparent point mutation and an underestimation of the true frequency of the indel. The *VAC6* strains had >300 called indels, so this artifact is non-trivial. The error will occur regardless of whether indel calling was attempted. VAMP provides algorithms for rectifying erroneous point mutation calls in the vicinity of indels by asking whether point mutations in reads not containing the indel can be rectified by introduction of indels observed in other nearby reads. An alternative strategy is to ignore bases within some distance of the ends of a read at the expense of discarding useful data.

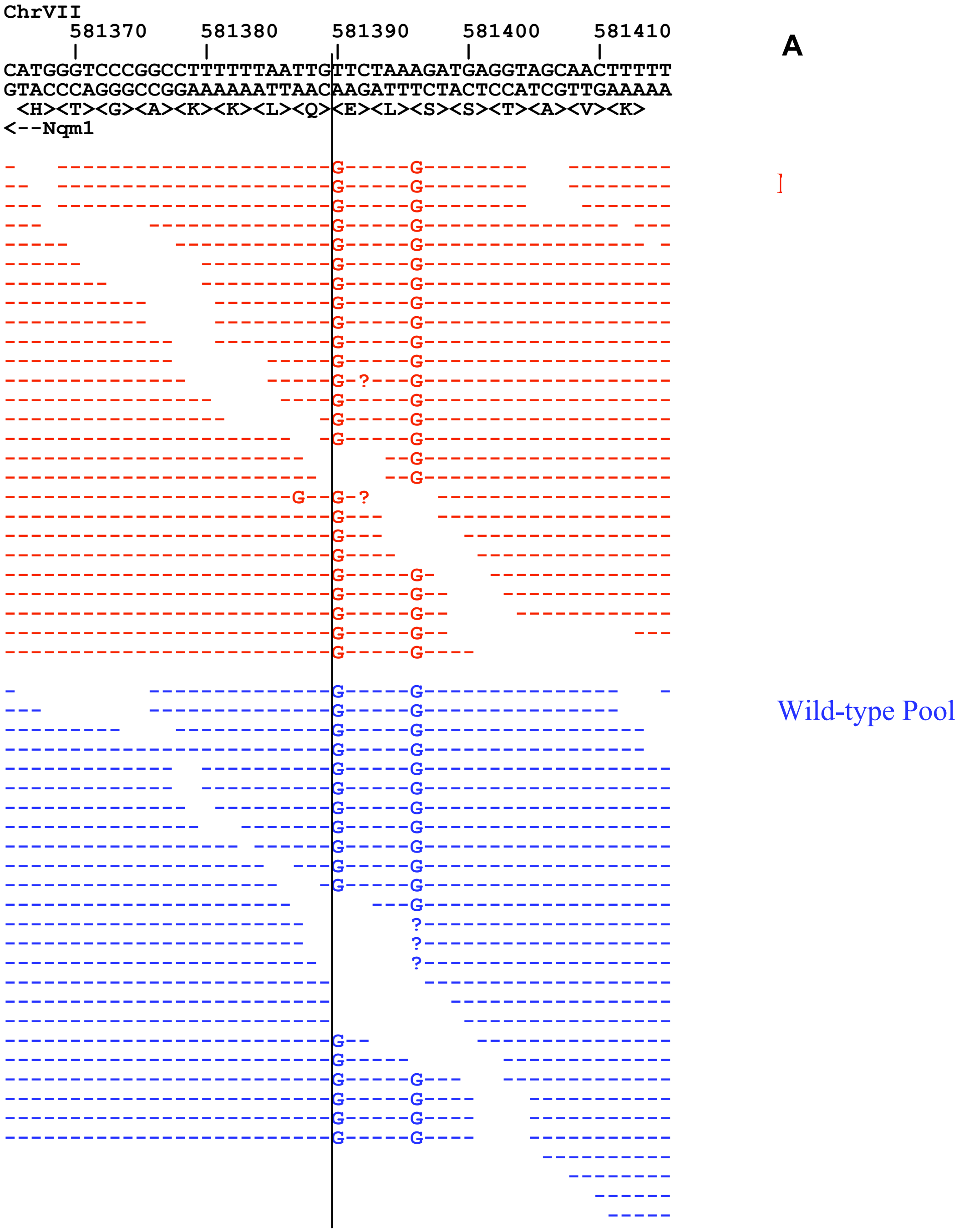
ChrVII
581370
581380
581390
581400
581410
CATGGGTCCCGGCCTTTTTTAATTGTTCTAAAGATGAGGTAGCAACTTTTT
GTACCCAGGGCCGGAAAAAATTAACAAGATTTCTACTCCATCGTTGAAAAA
<H><T><G><A><K><K><L><Q><E><L><S><S><T><A><V><K>
<--Nqm1
A
Wild-type Pool

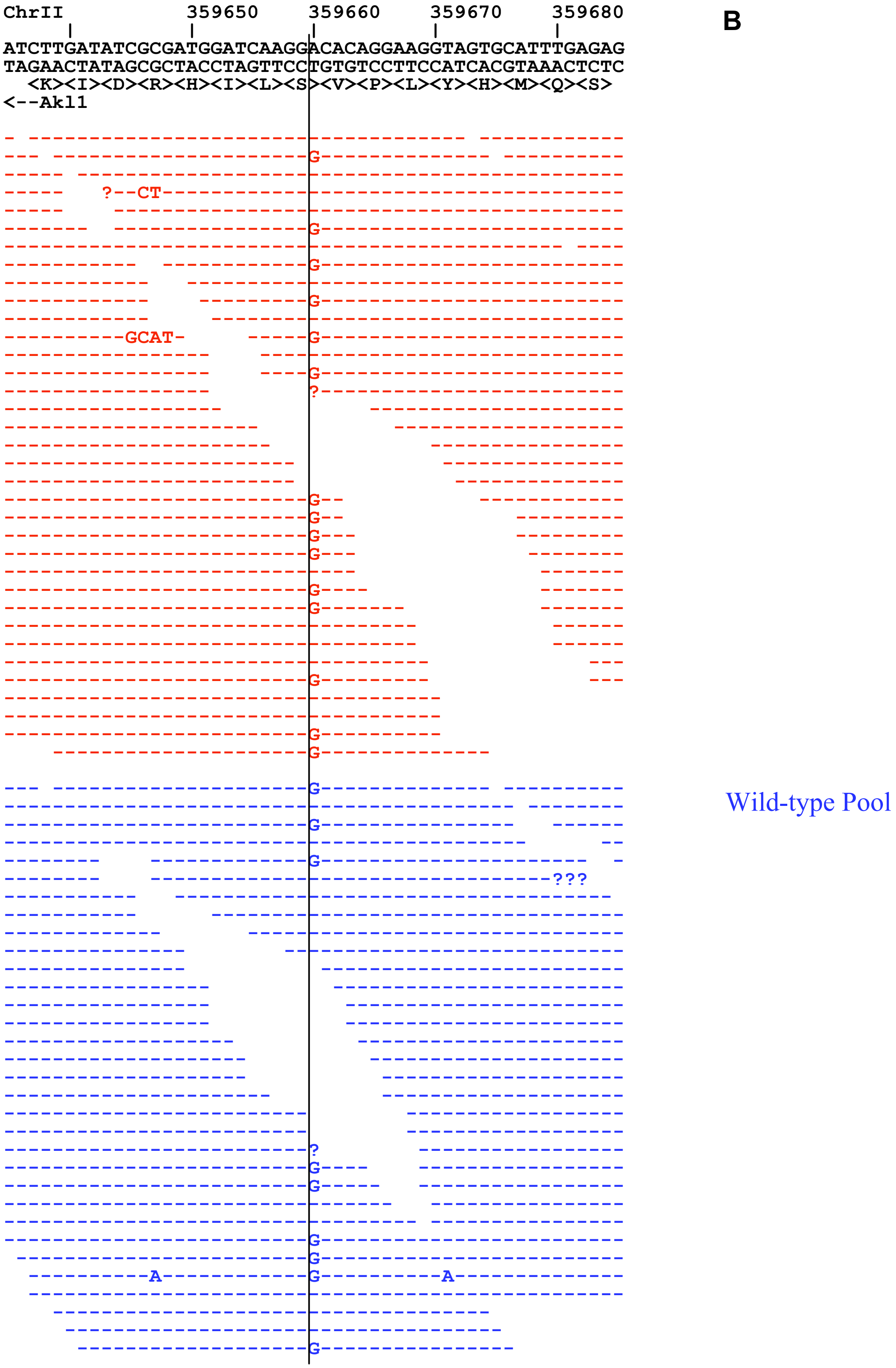
B
ChrII
359650
359660
359670
359680
ATCTTGATATCGCGATGGATCAAGGACACAGGAAGGTAGTGCATTTGAGAG
TAGAACTATAGCGCTACCTAGTTCCTGTGTCCTTCCATCACGTAAACTCTC
<K><I><D><R><H><I><L><S><V><P><L><Y><H><M><Q><S>
<--Akl1
?--CT
GCAT
Wild-type Pool
???
A

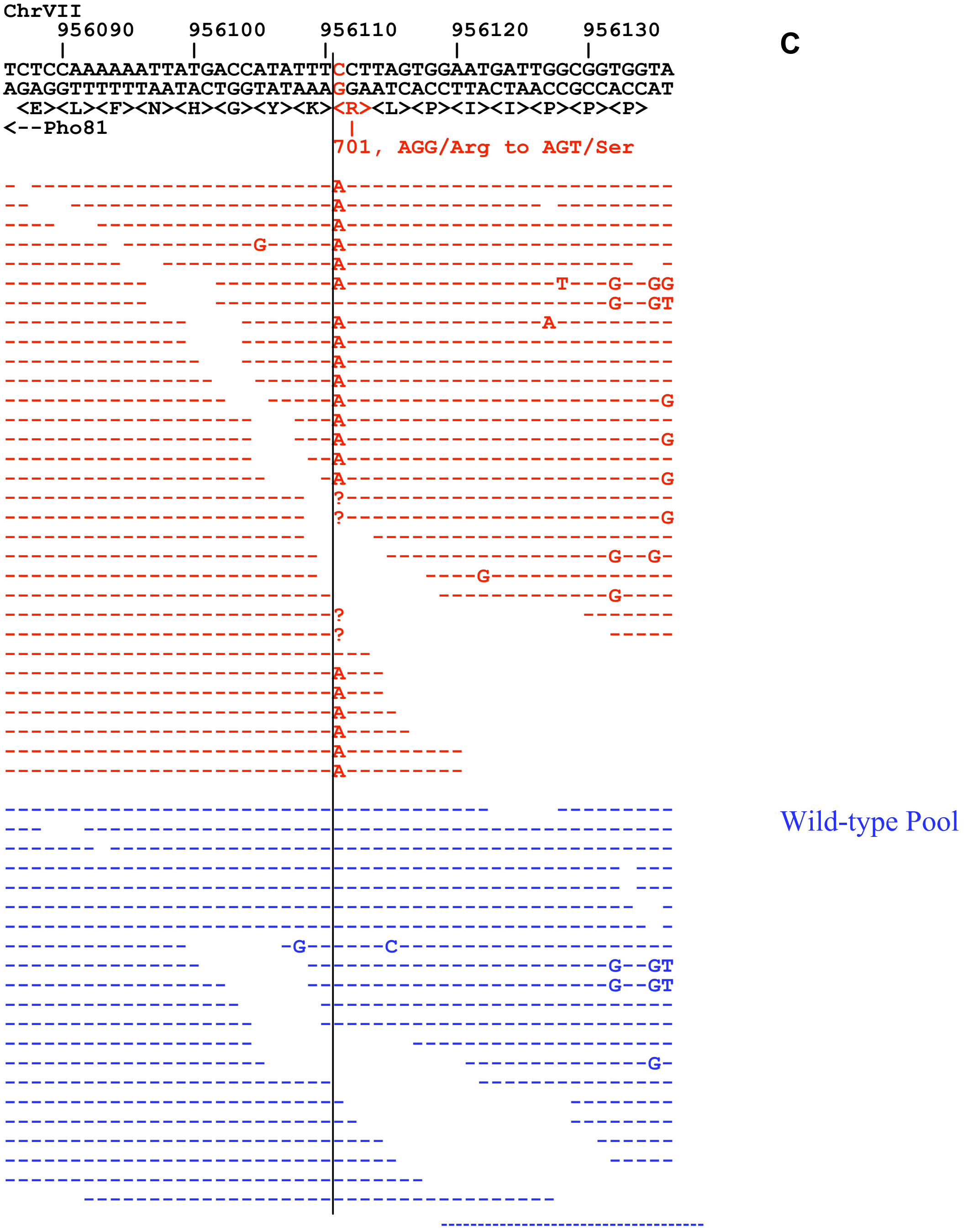
ChrVII
956090
956100
956110
956120
956130
TCTCCAAAAAATTATGACCATATTTCCTTAGTGGAATGATTGGCGGTGGTA
AGAGGTTTTTTAATACTGGTATAAAGGAATCACCTTACTAACCGCCACCAT
<E><L><F><N><H><G><Y><K><R><L><P><I><I><P><P><P>
<--Pho81
701, AGG/Arg to AGT/Ser
C
Wild-type Pool

FIGURE S5.—Mutation examples, including *PHO81-R701S.* For all panels, all sequence reads are shown that crossed the called mutation indicated by a vertical line. Because duplicate read pairs were purged all displayed reads are independent. Upper sequence lines show the sacCer2 reference genome and translation of any associated gene. Read bases are indicated with '-' if they matched the reference, or with the called base when different. Bases are indicated as '?' if they were ambiguous or represent mismatched bases at the ends of reads, given that PASS does not report the value of such bases. Terminal mismatches were accepted as consistent with a mutation that was otherwise positively called at a position. Base mismatches that occur in a minority of reads are interpreted as sequencing errors. Mutant pool reads are in red, wild-type pool reads in blue. (A) A randomly selected mutation predicted to be homozygous in the backcross diploid. The display fortuitously also captured a second homozygous mutation. (B) A randomly selected heterozygous mutation. (C) *PHO81-R701S. PHO81* is on the bottom genome strand and thus translation occurs in the reverse direction.

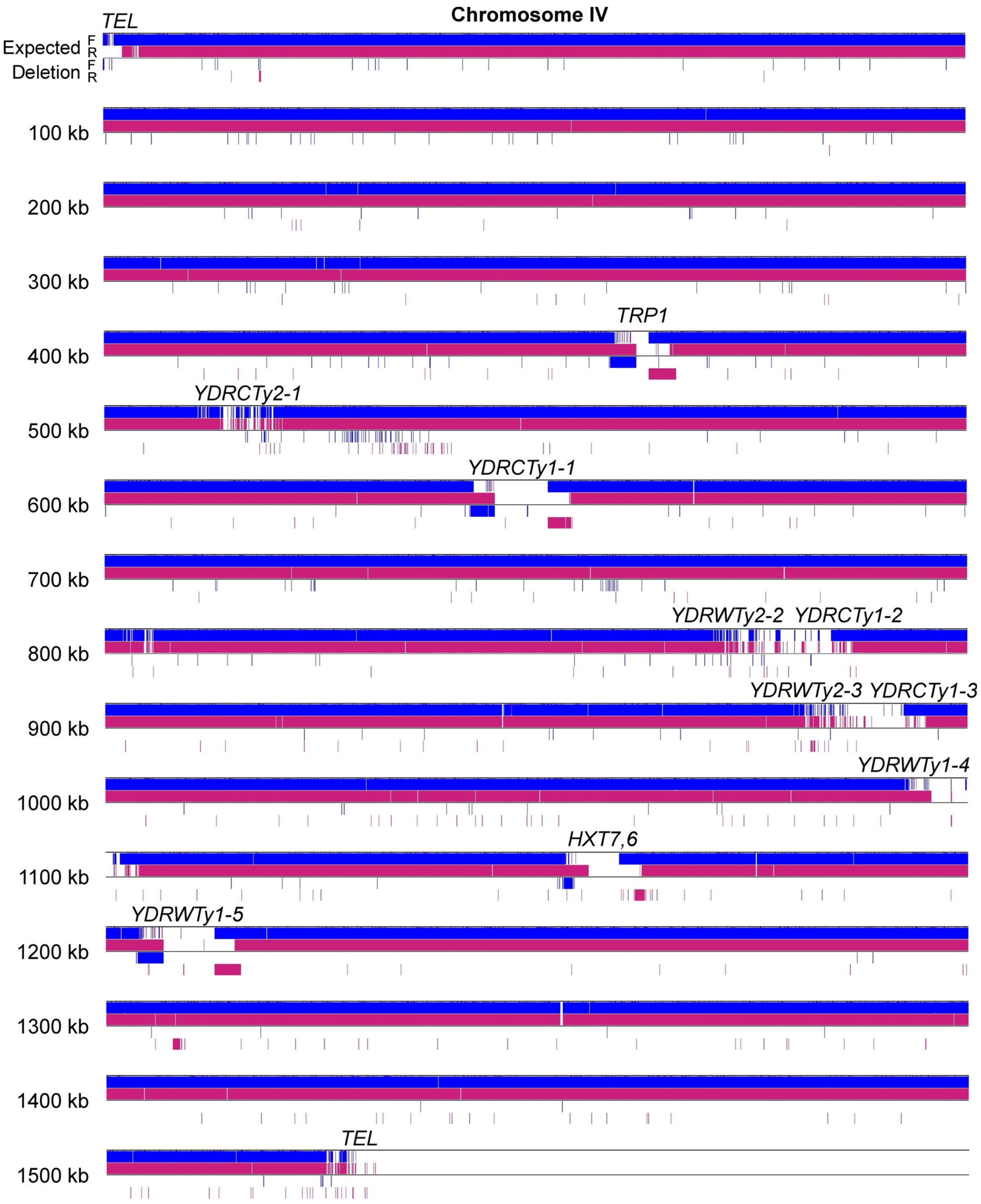

FIGURE S6.—Chromosome-wide view of all expected and deletion reads. Similar to Figures 6-8, now showing the entirety of chromosome IV to demonstrate the consistency of genome coverage in most regions and the ease of identifying the aberrant regions presented in Results. The only other notably aberrant mappings are in the subtelomeric DNA. Highly repetitive regions such as these and the rDNA array are not easily mapped, although by comparing different strains it is likely that these data could be mined for structural alterations.

A

```
   |36430    |36440    |36450                        ChrIX
AGATACCGTACGGAGGTCTGAATTCgCagCg                      as sequenced
AGATACCGTACGGAGGTCTGAATTCCCTACAGAAGTAGCTGTAAAAATTCA  reference
-------------------------?
-------------------------G-
-------------------------G-
-------------------------G-
-------------------------G-?
-------------------------G-?
-------------------------G-?
-----------T-------------G-?
-------------------------G-?
-------------------------G-?
-------------------------G-??
-------------------------G-??
-------------------------G-??
-------------------------G-AG-
-------------------------G-CG-
-------------------------G-AG-?
-------------------------G-AG-?
-------------------------G-AG-?
----------------G--------G-AG--
-------------------------G-AG-?-
-------------------------G-AG-G--
-------------------------G-AG-G--
-------------------------G-AG-G--
-------------------------G-AG-G--
```

B

```
                        |40810    |40820    |40830   ChrIX
                       gTcTGAATTCGCAGCGAACTCGTCTTGA  as sequenced
TTTTTCGCCTTGTAAGCTTTTTGATATGAATTCGCAGCGAACTCGTCTTGA  reference
                    ??-G-C-------------------------
                    ??-G-C-------------------------
                    ??-G-C-------------------------
                    ??-G-C-------------------------
                     ?-G-C-------------------------
                     ?-G-C-------------------------
                      -G-C-------------------------
                       ?-C-------------------------
                       ?-C-------------------------
                       --C-T-----------------G-----
                        -C-------------------------
                        -C?------------------------
                        -C-------------------------
                         ?-------------------------
```

C

```
AGATACCGTACGGAGGTCTGAATTCgCagCg              left end,  as sequenced (from A)
               ||||||||||||||||
               gTcTGAATTCGCAGCGAACTCGTCTTGA  right end, as sequenced (from B)
```

D

```
AGATACCGTACGGAGGTCTGAATTCCCTACAGAAGTAGCTGTA  left end reference
||||||||||||||||||||||||| |  |  |     ||  |
AGATACCGTACGGAGGTCTGAATTCGCAGCGAACTCGTCTTGA  junction as sequenced (from C)
       |      | | |||||||||||||||||||||||||
CTTGTAAGCTTTTTGATATGAATTCGCAGCGAACTCGTCTTGA  right end reference

               microhomology
```

FIGURE S7.—Sequence of the ChrIX *suc2-D9* deletion junction. (A) and (B) show the reads that cross the inferred deletion breakpoints on the left and right sides, respectively, annotated as in Figure S5. Note the presence of numerous mismatch calls at the extreme limits (bases highlighted in red in the consensus read sequences at the top). These mismatches arise because the bases have crossed the deletion junction and should be mapped to the other side of the deletion, as shown in (C) by aligning the left and right consensus sequences. Merging these in (D) reveals the sequence of the deletion junction, which shows a 7-bp

microhomology when compared to the reference genome, corresponding to an *Eco*RI site perhaps used in experimental construction of the allele.

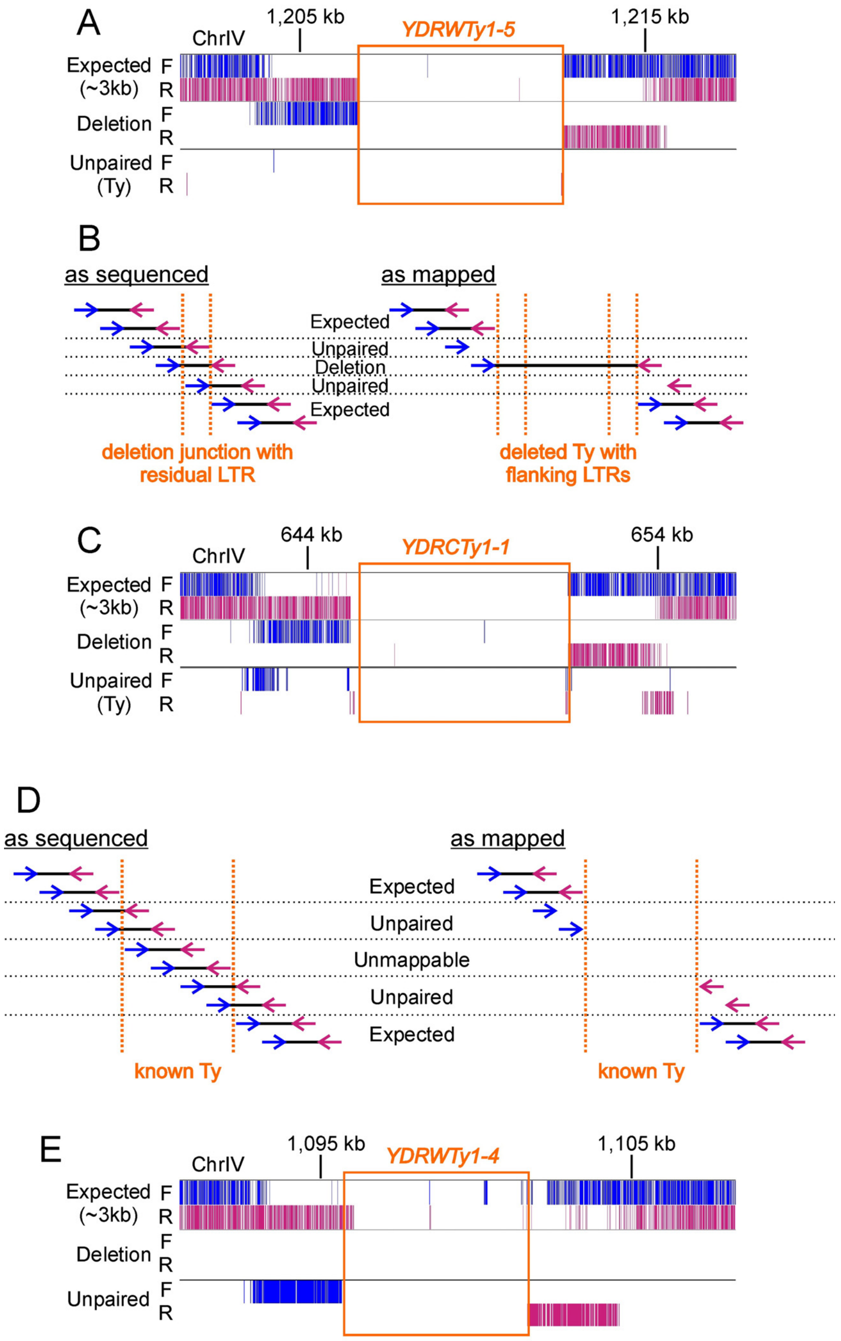

FIGURE S8.—Ty chromosome deletions. (A) Simple deletion of Ty element *YDRWTy1-5*, analogous to Figure 6A and drawn similarly to Figures 6B and 7C. (B) Similar to Figure 6C, showing the expected pattern of reads surrounding a Ty element deletion in which an LTR remains residual at the locus. (C) Deletion of Ty element *YDRCTy1-1* that shows unpaired reads consistent with the presence of an LTR. (D) and (E) For comparison, the expected and observed read patterns are shown for an annotated Ty element that was found to be present in the sequenced strain. Reads that fall within such a Ty element could theoretically be mapped as expected fragments, but in practice they cannot be because there are too many matching Ty sites throughout the genome, given that the analysis only allowed 10 mappings per read. Thus, unpaired reads are expected adjacent to the Ty element, as well as an absence of expected reads within the Ty. Deletion reads are notably absent, however.

```
TCATGGTAGCGCCTGTGCTTCGGTTACTTCTAAGGAAGTCCACACAAATCAAGATCCGTTAGACGTTTCAGCTTCCAAAACAGAAGAATGTGAGAAG
GCTTCCACTAAGGCTAACTCTCAACAGACAACAACACCTGCTTCATCAGCTGTTCCAGAGAACCCCCATCATGCCTCTCCTCAACCTGCTTCAGTAC
CACCTCCACAGAATGGGCCGTACCCACAGCAGTGCATGATGACCCAAAACCAAGCCAATCCATCTGGTTGGTCATTTTACGGACACCCATCTATGAT
TCCGTATACACCTTATCAAATGTCGCCTATGTACTTTCCACCTGGGCCACAATCACAGTTTCCGCAGTATCCATCATCAGTTGGAACGCCTCTGAGC
ACTCCATCACCTGAGTCAGGTAATACATTTACTGATTCATCCTCAGCGGACTCTGATATGACATCCACTAAAAAATATGTCAGACCACCACCAATGT
TAACCTCACCTAATGACTTTCCAAANNNNNNNNNNNNNNNNNNNNNNNNNNNNNNNNNNNNNNNNNNNNNNNNNNNNNNNNNNNNNNNNNNNNNNNNNN
NNNNNNNNNNNNNNNNNNNNNNNNNNNNNNNNNNNNNNNNNNNNNNNNNNNNNNNNNNNNNNNNNNNNNNNNNNNNNNNNNNNNNNNNNNNATTATT
CCGACAGTAAACGGAAAACCCGTACGTCAGATCACTGATGATGAACTCACCTTCTTGTATAACACTTTTCAAATATTTGCTCCCTCTCAATTCCTAC
CTACCTGGGTCAAAGACATCCTATCCGTTGATTATACGGATATCATGAAAATTCTTTCCAAAAGTATTGAAAAAATGCAATCTGATACCCAAGAGGC
AAACGACATTGTGACCCTGGCAAATTTGCAATATAATGGCAGTACACCTGCAGATGCATTTGAAACAAAAGTCACAAACATTATCGACAGACTGAAC
AATAATGGCATTCATATCAATAACAAGGTCGCATGCCAATTAATTATGAGAGGTCTATCTGGCGAATATAAATTTTTACGCTACACACGTCATCGAC
ATCTAAATATGACAGTCGCTGAACTGTTCTTAGATATCCATGCTATTTATGAAGAACAACAGGGATCGAGAAACAGTAAACCTAATTACAGGAGAAA
TCCGAGTGATGAGAAGAATGATTCTCGCAGCTATACGAATACAACCAAACCCAAAGTTATAGCTCGGAATCCTCAAAAAACAAATAATTCGAAATCG
AAAACAGCCAGGGCTCACAATGTATCCACATCTAATAACTCTCCCAGCACGGACAACGATTCCATCAGTAAATCAACTACTGAACCGATTCAATTGA
ACAATAAGCACGACCTTCATCTTAGGCCAGAAACTTACTGAATCTACAGTAAATCATACTAATCATTCTGATGATGAACTCCCTGGACACCTCCTTC
TCGATTCAGGAGCATCACGAACCCTTATAAGATCTGCTCATCACATACACTCAGCATCATCTAATCCTGACATAAACGTAGTTGATGCTCAAAAAAG
AAATATACCAATTAACGCTATTGGTGACCTACAATTTCACTTCCAGGACAACACCAAAACATCAATAAAGGTATTGCACACTCCTAACATAGCCTAT
GACTTACTCAGTTTGAATGAATTGGCTGCAGTAGATATCACAGCATGCTTTACCAAAAACGTCTTAGAACGGTCTGACGGCACTGTACTTGCACCTA
TCGTAAAATATGGAGACTTTTACTGGGTATCTAAAAAGTACTTGCTTCCATCAAATATCTCCGTACCCACCATCAATAATGTCCATACAAGTGAAAG
TACACGCAAATATCCTTATCCTTTCATTCATCGAATGCTTGCGCATGCCAATGCACAGACAATTCGATACTCACTTAAAAATAACACCATCACGTAT
TTTAACGAATCAGATGTCGACTGGTCTAGTGCTATTGACTATCAATGTCCTGATTGTTTAATCGGCAAAAGCACCAAACACAGACATATCAAAGGTT
CACGACTAAAATACCAAAATTCATACGAACCCTTTCAATACCTACATACTGACATATTTGGTCCAGTTCACAACCTACCAAAAAGTGCACCATCCTA
TTTCATCTCATTTACTGATGAGACAACAAAATTCCGTTGGGTTTATCCATTACACGACCGTCGCGAGGACTCTATCCTCGATGTTTTTACTACGATA
CTAGCTTTTATTAAGAACCAGTTTCAGGCCAGTGTCTTGGTTATACAAATGGACCGTGGTTCTGAGTATACTAACAGAACTCTCCATAAATTCCTTG
AAAAAAATGGTATAACTCCATGCTATACAACCACAGCGGATTCCCGAGCACATGGAGTCGCTGAACGGCTCAACCGTACCTTATTAGATGACTGCCG
TACTCAACTGCAATGTAGTGGTTTACCGAACCATTTATGGTTCTCTGCAATCGAATTTTCTACTATTGTGAGAAATTCACTAGCTTCACCTAAAAGC
AAAAAATCTGCAAGACAACATGCTGGCTTGGCAGGACTTGATATCAGTACTTTGTTACCTTTCGGTCAACCTGTTATCGTCAATGATCACAACCCTA
ACTCCAAAATACATCCTCGTGGCATCCCAGGCTACGCTCTACATCCGTCTCGAAACTCTTATGGATATATCATCTATCTTCCATCCTTAAAGAAGAC
NNNNNNNNNNACTAACTATGTTATTCTTCAGGGCAAGGAATCCAGATTAGATCAATTCAATTANNACGCACTCACTTTCGATGAAGACTTAAACCGT
TTAACTGCTTCATATCAATCGTTCATTGCGTCAAATGAGATCCAACAATCCGATGATCTTAACATAGAATCTGACCATGACTTCCAATCTGACATCG
AACTACATCCTGAGCAACCGAGAAATGTCCTTTCAAAAGCTGTGAGTCCAACCGATTCCACACCTCCGTCAACTCATACTGAAGATTCGAAACGTGT
TTCTAAAACCAATATTCGCGCACCCAGAGAAGTTGACCCCAACATATCTGAATCTAATATTCTTCCATCAAAGAAGAGATCTAGCACCCCCCAAATT
TCCAATATCGAGAGTACCGGTTCGGGTGGTATGCATAAATTAAATGTTCCTTTACTTGCTCCCATGTCCCAATCTAACACACATGAGTCGTCGCACG
CCAGTAAATCTAAAGATTTCAGACACTCAGACTCGTACAGTGAAAATGAGACTAATCATACAAACGTACCAATATCCAGTACGGGTGGTACCAACAA
CAAAACTGTTCCGCAGATAAGTGACCAAGAGACTGAGAAAAGGATTATACACCGTTCACCTTCAATCGATGCTTCTCCACCGGAAAATAATTCATCG
CACAATATTGTTCCTATCAAAACGCCAACTACTGTTTCTGAACAGAATACCGAGGAATCTATCATCGCTGATCTCCCACTCCCTGATCTACCTCCAG
AATCTCCTACCGAATTCCCTGACCCATTTAAAGAACTCCCACCGATCAATTCTCGTCAAACTAATTCCAGTTTGGGTGGTATTGGTGACTCTAATGC
CTATACTACTATCAACAGTAAGAAAAGATCATTAGAAGATAATGAAACTGAAATTAAGGTATCACGAGACACATGGAATACTAAGAATATGCGTAGT
TTAGAACCTCCGAGATCGAAGAAACGAATTCACCTGATTGCAGCTGTAAAAGCAGTAAAATCAATCAAACCAATACGGACAACCTTACGATACGATG
AGGCAATCACCTATAATAAAGATATTAAAGAAAAAGAAAAATATATCGAGGCATACCACAAAGAAGTCAATCAACTGTTGAAGATGAAAACTTGGGA
CACTGACGAATATTATGACAGAAAAGAAATAGACCCTAAAAGAGTAATAAACTCAATGTTTATCTTCAACAAGAAACGTGACGGTACTCATAAAGCT
AGATTTGTTGCAAGAGGTGATATTCAGCATCCTGACACTTACGACTCAGGCATGCAATCCAATACCGTACATCACTATGCATTAATGACATCCCTGT
CACTTGCATTAGACAATAACTACTATATTACACAATTAGACATATCTTCGGCATATTTGTATGCAGACATCAAAGAAGAATTATACATAAGACCTCC
ACCACATTTAGGAATGAATGATAAGTTGATACGTTTGAAGAAATCACTTTATGGATTGAAACAAAGTGGAGCGAACTGGTACGAAACTATCAAATCA
TACCTGATACAACAATGTGGTATGGAAGAAGTTCGTGGATGGTCATGCGTATTTAAAAACAGTCAAGTGACAATTTGTTTATTCGTAGATGATATGG
TATTGTTTAGCAAAAATCTAAATTCAAACAAAAGAATTATANNNNNNNNNNNNNNNNNNNNNNNNNNNNNNNNNNNNNNNNNNNNNNNNNNNNNNNN
NNNNNTTCAATATGACATTCTTGGCTTGGAAATCAAATACCAAAGAGGTAAATACATGAAATTGGGTATGGAAAACTCATTAACTGAAAAAATACCC
AAACTAAACGTACCTTTAAACCCAAAAGGAAGGAAACTTAGTGCTCCAGGTCAACCAGGTCTATATATAGACCAGCAAGAACTAGAGCTAGAAGAAG
ATGATTACAAAATGAAGGTACATGAAATGCAAAAGCTGATAGGTCTAGCATCATATGTTGGATATAAATTTAGATTTGACCTATTATACTACATCAA
CACACTTGCACAACATATACTATTTCCGTCCAAGCAAGTGTTAGATATGACATATGAATTGATACAGTTCATATGGAATACGAGAGATAAGCAATTA
ATATGGCACAAAAGCAAACCTGTTAAGCCAACAAATAAATTAGTTGTTATAAGCGATGCCTCGTATGGCAACCAACCGTATTATAAATCACAAATTG
GCAACATATATTTACTTAATGGAAAGGTAATTGGAGGAAAGTCCACCAAGGCTTCATTAACATGTACTTCAACTACGGAAGCAGAAATACACGCGAT
AAGTGAATCTGTCCCATTATTAAATAATCTAAGTTACCTGATACAAGAACTTGACAAGAAACCAATTACCAAAGGATTACTAACCGACAGTAAATCT
ACAATCAGTATAATTATATCCAATAATGAAGAGAAATTTAGGAACAGATTTTTTGGTACTAAAGCAATGAGATTGAGAGATGAAGTATCAGGAAATC
ATCTGCACGTATGCTATATCGAAACCAAAAAGAATATTGCAGACGTAATGACCAAACCTCTTCCGATAAAAACATTCAAACTATTAACAAACAAATG
GATTCATTAGATCTATTACATTATGGGTGGTATGTTGGAATAAAAATCCACTATCGTCTATCAACTAATAGTTATATTATCAATATATTATCATATA
CGGTGTTAAGATGANNNNNNNAGTTATGAGAAGCTGTCATCGAAGTTAGAGGAAGCTGAAACGCAAGGATTGATAATGTAATAGGATCAATGAATAT
ATAAAACGGAATGAGGAATAATCGTAATATTAGTATGTAGAAATATAGATTCCATTTTGAGGATTCCTATATCCTCGAGGAGAACTTCTAGTATATT
CTGTATACCTAATATTATAGCCTTTATCAACAATGGAATC
```

FIGURE S9.—Sequence of the novel *UBC4* Ty element insertion. The contig was built by assembly of LWY10741 sequence reads onto a Ty scaffold corresponding to *YHRCTy1-1*. Sequence differences were iteratively changed to those determined by the LWY10741 reads until convergence was observed. *YHRCTy1-1* bases that were not mapped by LWY10741 reads are indicated as 'N'. Isolated N's most likely represent coverage holes, while large blocks of N's might represent sequences absent from the *UBC4* Ty.

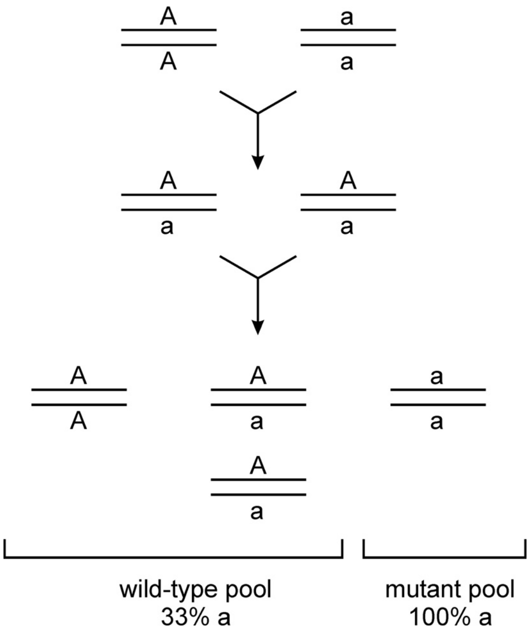

FIGURE S10.—Extension of pooled crosses to a mammalian system. When the organism under study is obligatorily diploid, pooled linkage analysis might still be applied as illustrated here for a target recessive mutation, a. The same relationship can be inferred in the final generation for human families in the absence of the ability to execute controlled crosses as in organisms such as mice.

TABLE S1

Called point mutations and indels in the *VAC6* pools

Table S1 is available for download as an Excel file at http://www.genetics.org/cgi/content/full/genetics.110.123232/DC1.

SUPPORTING REFERENCES

CAMPAGNA, D., A. ALBIERO, A. BILARDI, E. CANIATO, C. FORCATO *et al.*, 2009 PASS: a program to align short sequences. Bioinformatics **25:** 967-968.

DEW, I. M., B. WALENZ and G. SUTTON, 2005 A tool for analyzing mate pairs in assemblies (TAMPA). J Comput Biol **12:** 497-513.

KORBEL, J. O., A. E. URBAN, J. P. AFFOURTIT, B. GODWIN, F. GRUBERT *et al.*, 2007 Paired-end mapping reveals extensive structural variation in the human genome. Science **318:** 420-426.

LANGMEAD, B., C. TRAPNELL, M. POP and S. L. SALZBERG, 2009 Ultrafast and memory-efficient alignment of short DNA sequences to the human genome. Genome Biol **10:** R25.